

AN ABSTRACT OF THE CAPSTONE REPORT OF

Yunhan Gao for the Degree of Master of Chemical Sciences

Title: Effect of the Anchoring Groups on the Photostability of Ruthenium(II) Polypyridyl Sensitizers

Project conducted at: Department of Chemistry
University of Pennsylvania
231 S. 34th Street, Philadelphia, PA 19104-6323
Supervisor: Thomas E. Mallouk
Dates of Project: May 22, 2020 – April 16, 2021

Abstract Approved:
Thomas E. Mallouk, principal investigator

Ruthenium(II) polypyridyl derivatives are widely used as sensitizer molecules in water-splitting dye-sensitized photoelectrochemical cells (WS-DSPECs) to harvest solar energy and generate hydrogen and oxygen gas from water. The desorption of sensitizer molecules from the TiO₂ surface during long-term illumination is a significant problem for the photostability of these cells. Another factor that limits the efficiency of the cells is the low injection yield from the dye excited state to the electrode at neutral pH. To address these two problems, the effects of different anchoring groups (carboxylate or phosphonate) at the 4,4'-positions of bipyridine were systematically studied. In this report, three ruthenium(II) polypyridyl sensitizers were synthesized and characterized. Results from stability measurements showed that the phosphonate anchoring groups can enhance the photostability of ruthenium(II) sensitizers over the pH range from 4.9 to 6.9 compared with carboxylate substitutions.

*Effect of the Anchoring Groups on the Photostability of
Ruthenium (II) Polypyridyl Sensitizers*

by
Yunhan Gao

A CAPSTONE REPORT
submitted to the
University of Pennsylvania

in partial fulfillment of
the requirements for
the degree of

Master of Chemical Sciences

Presented on April 16, 2021
Commencement on May 17, 2021

Master of Chemical Sciences Capstone Report of Yunhan Gao Presented on April 16, 2021.

APPROVED:



Prof. Thomas E. Mallouk, Representing Materials Chemistry

I understand that my Capstone Report will become part of the permanent collection of the University of Pennsylvania Master of Chemical Sciences Program. My signature below authorizes the release of my final report to any reader upon request.



Yunhan Gao, Author

Acknowledgments

I would like to thank my research advisor, Professor Thomas Mallouk for providing me opportunities, support and instructions. I sincerely appreciate my mentor Langqiu Xiao for guiding me in the research. Special thanks to my committee members Professor Neil Tomson and Dr. Ana-Rita Mayol for their efforts and advice on my project. I would like to extend my gratitude to all my group members for providing a warm atmosphere. Special thanks to my family who let me know I am not alone.

Table of Contents

Abstract.....	i
Approval page.....	ii
Acknowledgments.....	iii
List of Figures.....	v
List of Tables.....	vi
List of Schemes.....	vii
List of Appendices.....	viii
Introduction.....	1
Materials and Methods.....	4
Results and Discussion.....	11
Conclusion and Future Work.....	20
References.....	21
Appendices.....	23

List of Figures

Figure 1. The structural design of a WS-DSPEC.....	1
Figure 2. Molecular structure of sensitizers 1 , 2 , and 3	3
Figure 3. A photograph of electrode (sensitizer 2) before and after desorption at pH 4.9.....	14
Figure 4. Absorbance of sensitizers at pH 4.9.....	16
Figure 5. Absorbance of sensitizers at pH 6.9.....	17
Figure 6. The optimized geometrical structure of sensitizer 1	19

List of Tables

Table 1. Summary of the results using carboxylate and phosphonate as anchors.....	2
Table 2. MLCT band positions of molecular sensitizers	14

List of Schemes

Scheme 1. The synthetic route of diphosphonate ester bipyridine ligand 4	11
Scheme 2. The synthetic route of complex 1	12
Scheme 3. The synthetic route of complex 3	13

List of Appendices

Appendix 1. ^1H NMR of 1	23
Appendix 2. ^{31}P NMR of 1	24
Appendix 3. ^1H NMR of 2	25
Appendix 4. ^1H NMR of 3	26
Appendix 5. ^{31}P NMR of 3	27
Appendix 6. ^1H NMR of 4	28
Appendix 7. ^{31}P NMR of 4	29
Appendix 8. ^1H NMR of 5	30
Appendix 9. ^{31}P NMR of 5	31
Appendix 10. ^1H NMR of 6	32
Appendix 11. ^1H NMR of 7	33
Appendix 12. ^1H NMR of 7	34
Appendix 13. ^1H NMR of 9	35
Appendix 14. ^1H NMR of 10	36
Appendix 15. ^1H NMR of 11	37
Appendix 16. ^{31}P NMR of 11	38

Introduction

Global energy consumption continues to grow rapidly, and it is expected to reach a level approximately two times greater than that of current consumption by 2050.¹ Fossil fuels will continue to be a major source of energy for the foreseeable future.² It is predicted that in the coming few decades, carbon dioxide generated from the combustion of fossil fuels will cause environmental and climatic problems.³ To alleviate these problems, solar energy conversion may be envisioned as a renewable source of energy that can be scaled to replace much of the current fossil fuel consumption. A key technological problem in this area is the conversion of solar electricity to fuel. The electrolysis of water to produce hydrogen has become a mature technology and a number of energy-dense liquid fuels have been made by the combination of this H₂ with CO₂ under catalytic conditions.⁴

Over the past decade, the Mallouk group has been focusing on identifying the sources of efficiency loss and improving the performance of water-splitting dye-sensitized photoelectrochemical cells (WS-DSPECs). The structural design is shown in **Figure 1**.⁵ The cell can absorb visible light energy and drive the catalytic reactions necessary to generate hydrogen and oxygen gas from water by using molecular sensitizers and catalysts.¹ As shown in the figure, water is oxidized at the photoanode of the dye cell to form oxygen gas, and protons are reduced to hydrogen at the cathode. A small external bias voltage is applied to drive the overall redox reaction. Since the major challenge in improving the efficiency and durability of water splitting cells is the catalytic four-electron oxidation of water, the oxygen evolution reactions (OER) on the anode side in the WS-DSPECs has attracted much interest and dominates research activities on this problem.⁵ Owing to the complexity of the cell, each component of the photoanode can affect the energy conversion efficiency of the cell and need to be optimized. One of the primary factors is the properties of molecular sensitizers. The ideal sensitizer requires not only a stable binding model to TiO₂ but also optimal electrochemical properties.

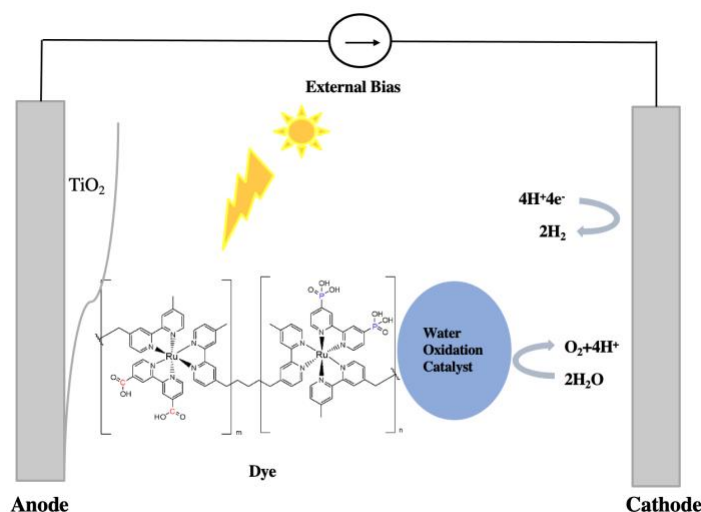
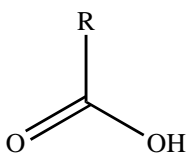
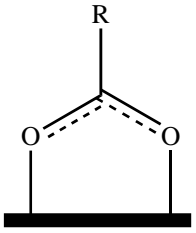
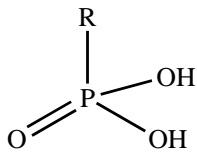
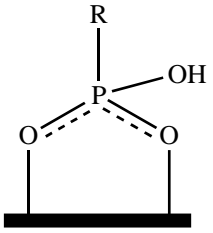


Figure 1. The structural design of a WS-DSPEC.⁵

Ruthenium(II) polypyridyl derivatives with intense metal-to-ligand charge transfer (MLCT) absorption in the visible region around 460 nm are widely used as molecular sensitizers in WS-DSPECs. Typically, anchoring groups like carboxylate and phosphonate are the most common substitutions at the 4,4'-positions of bipyridine ligands (**Table 1**). The phosphonate groups bind to a TiO₂ surface by the κ^2 bridging mode shown in **Table 1** at neutral pH (~7), but while the carboxylate groups bind in a similar fashion, they only exhibit hydrolytic stability at low pH (~4.9).⁶ At higher pH, the hydrolysis of carboxylate groups can lead to the release of adsorbed sensitizers from metal dioxide surfaces. On the contrary, carboxylate groups, instead of the phosphate, are expected to promote more rapid charge injection. The time constant for electron injection from the ligand to the TiO₂ conduction band is much smaller for the carboxylate anchors (13 fs for the carboxylate and 28 fs for the phosphonate).⁷ Because the phosphonate anchoring group gives a higher stability binding to metal oxides and the carboxylate is known to exhibit more favorable photoinjection rates, a ruthenium sensitizer containing both substitutions may provide both stability with respect to hydrolysis at neutral pH and fast electron injection rates.

Table 1. Summary of using carboxylate and phosphonate as anchors including the preferred binding mode, pH stability range, relative electron injection efficiency

Anchoring Group	Binding Mode	Stability Range	Electron Injection
		pH < 4	efficient
		pH < 7	moderate

To explore the effect of anchoring groups on the sensitizers, this project develops three ruthenium(II) complexes (**Figure 2**). These molecular sensitizers have similar structures with different anchoring groups at the 4,4'-positions of bipyridine ligands. Sensitizer **1** (RuP-RuP) and **2** (RuC-RuC) have only one type of anchoring group (carboxylate or phosphonate substitution), while **3** (RuC-RuP) combines both. The long-term photostability of the molecular sensitizers will be measured from pH 4.9 to pH 6.9 under constant irradiation (10 mW/cm²). In order to measure the photostability of sensitizers on

the electrode surface, this project consists of three parts: the synthesis of ruthenium(II) sensitizers, the photostability measurements and the theoretical geometry optimization of sensitizer **1**. Two types of anchors will be focused and synthesized in this study. They differed from the substitution groups (carboxylate or phosphonate) at the 4,4'-positions of bipyridine. In order to study the stability influence from these two groups, three ruthenium(II) complexes (**1**, **2** and **3**) with different types of anchors are synthesized via a commonly synthetic route.⁴ In the previous study, the Mallouk group compared the performance of the monomeric and oligomeric sensitizers.⁵ It was found that the longer length of the sensitizers dramatically improved the stability on the metal dioxide surface. The monomeric sensitizers with phosphonate or carboxylate anchors show a poor photostability. Therefore, the sensitizers with two ruthenium metal centers are focused on this project as they have a longer length but with a simple structure. Due to the symmetric structure of the sensitizer, the outer unit containing phosphonate and carboxylate groups will be synthesized firstly, then coupled with the inner linker (color in blue) to achieve the target structure. Structures of sensitizers are confirmed by nuclear magnetic resonance spectroscopy (NMR) and liquid chromatography–mass spectrometry (LC–MS). The photostability of the sensitizers will be measured by illuminating the electrode under constant irradiation (10 mW/cm^2), and the absorption change is monitored by UV-Vis. The density functional theory (DFT) approach will be focused to investigate absorption manners of sensitizers anchored to TiO_2 surface. Through the theoretical studies, how the number of anchors (phosphonate or carboxylate groups) affect the binding stability on TiO_2 will be illustrated to further support the experimental data. The geometry optimization of complex **1**, the first step of the theoretical study, is partly finished.

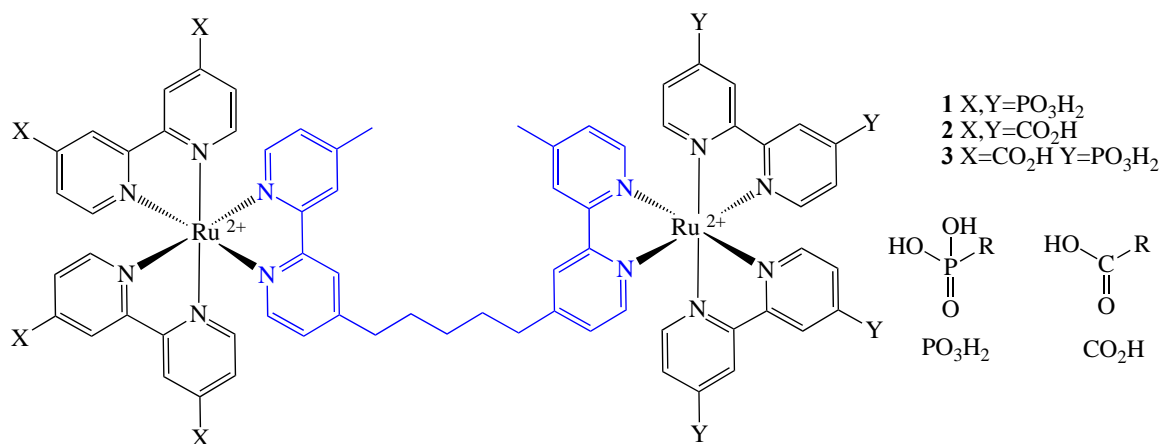


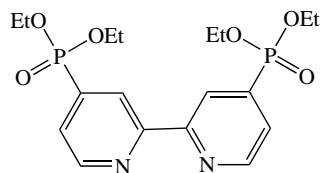
Figure 2. Molecular structure of sensitizers **1**, **2**, and **3**

Materials and Methods

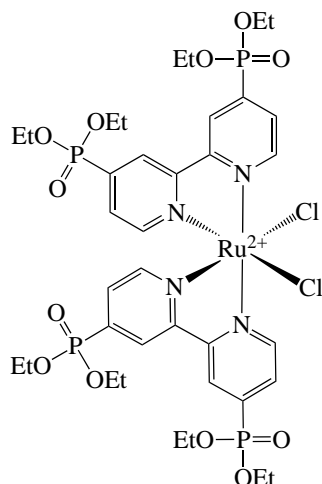
Materials

Triphenylphosphine (99%), sodium chloride (99%), and ammonium hydroxide solution (99.99%) were purchased from Sigma-Aldrich. Triethylamine (99%), lithium chloride (99%), and tetrakis(triphenylphosphine)palladium(0) (99%) were purchased from Acros Organics. 4,4'-dibromo-2,2'-bipyridine (98%) was purchased from Astatech. 1,3-dibromopropane (98%), and 4,4'-dimethyl-2,2'-dipyridyl (98%) were purchased from TCI America. Diethyl phosphite (97%) was purchased from Alfa Aesar. All reagents were used as received. Sephadex LH-20 was purchased from GE Healthcare. Sephadex LH-20 is swelled in MeOH for at least 3 hours at room temperature before loading into the column. Methanol-*d*₄ (D, 99.8%), chloroform-*d* (D, 99.8%) were purchased from Cambridge Isotope Laboratories. Chemical shifts (δ) are reported in parts per million (ppm) relative to the solvent reference. The peak assignments are reported as following: chemical shift, multiplicity (s = singlet, d = doublet, t = triplet, dd = doublet of doublet, m = multiplet), integration. Liquid chromatography - mass spectra (LC-MS) was at the University of Pennsylvania Mass Spectroscopy Service Center. The UV-Vis spectra were recorded at 25 °C on a Varian Cary 6000i and Agilent Cary 60 UV-Vis spectrometer using 1 cm quartz cuvettes.

General methods for the synthesis of Sensitizer 1 (RuP-RuP)

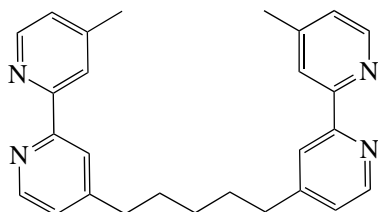


4,4'-bis(diethylphosphonate)-2,2'-bipyridine, 4. Compound **4** was synthesized according to Neuthe's procedure.⁹ 4,4'-dibromo-2,2'-bipyridine (1.22 g, 3.88 mmol) was dissolved in a mixture of triethylamine (1.3 mL) and dry toluene (70 mL) under an inert atmosphere (Ar). Diethyl phosphite (1.15 mL, 8.92 mmol), tetrakis(triphenylphosphine)palladium(0) (0.450 g, 0.400 mmol) and triphenylphosphine (10.2 g, 38.8 mmol) were then added. The solution was refluxed at 110 °C for 6 hours. Toluene (10 mL) was added after cooling to room temperature, causing the gel-like precipitate that had formed during the reaction to dissolve. The resulting solution was washed with a mixture of saturated NH₄OH (3 x 30 mL), and the organic layer was dried with anhydrous MgSO₄. The solvent was evaporated to afford an off-white powder. The crude product was purified by silica-gel column chromatography (in a column h = 30 cm, d = 15 mm). Dichloromethane was used as the initial eluent to remove the triphenylphosphine, followed by a mixture of methanol and dichloromethane in the volume ratio of 3:100. The second eluate was collected and evaporated to yield a white powder. Yield: 283 mg (70%). ¹H NMR (500 MHz, methanol-*d*₄): δ = 8.34 (t, 2H), 8.27 (d, 2H), 7.76 (dd, 2H), 3.69 (m, 8H), 0.85 ppm (t, 12H); ³¹P NMR (202 MHz, *d*₄-MeOD): δ = 14.61 ppm (s).

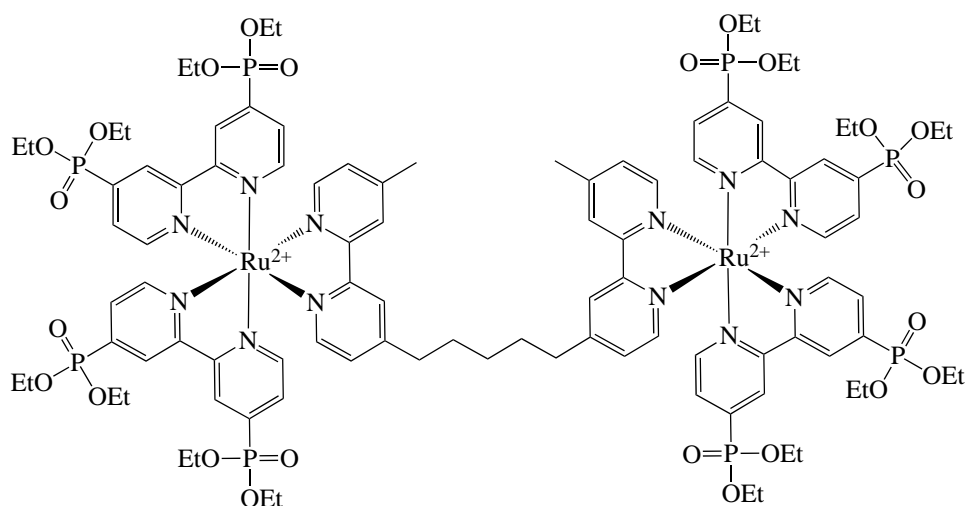


***cis*-Dichloro-bis(4,4'-bis(ethylphosphonate)-2,2'-bipyridine)ruthenium, 5.**

Dichlorotetrakis(dimethylsulfoxide) ruthenium(II) (205 mg, 0.423 mmol), bipyridine ligand **4** (362 mg, 0.846 mmol), and LiCl (286 mg, 6.8 mmol) were dissolved in dry *N,N*-dimethylformamide (10 mL). The mixture was heated at 160 °C for 6 hours under an inert atmosphere (Ar) in the dark. DCM (10 mL) was added after cooling to room temperature, and the precipitate was filtered. After washing with DCM, the compound was dried in a vacuum and used without further purification.¹⁰ Yield: 347.8 mg (80%). ¹H NMR (500 MHz, *d*₄-MeOD): δ = 10.06 (dd, 2H), 8.87 (dd, 2H), 8.84 (d, 2H), 8.60 (d, 2H), 7.68 (dd, 2H), 7.32 (dd, 2H), 4.35 (m, 8H), 4.19 (m, 8H), 1.47 (t, 12H), 1.33 ppm (t, 12H); ³¹P NMR (202 MHz, *d*₄-MeOD): δ = 7.09 ppm (s).



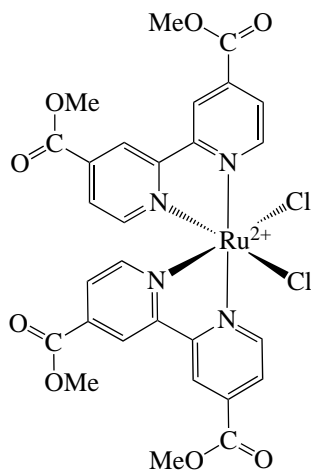
1,5-bis-(4-methyl-2,2'-bipyridyl-4-yl)pentane, 6. The linker **6** was synthesized according to Mulyana's route.¹¹ 4,4'-Dimethyl-2,2'-dipyridyl (1.60 g, 8.7 mmol) was dissolved in dry tetrahydrofuran (250 mL) under an inert atmosphere (Ar) and then the solution was cooled to -78 °C (dry ice/acetone bath). Lithium diisopropylamide (1.03 g, 9.6 mmol) in tetrahydrofuran/hexanes was added dropwise over 30 minutes. After stirring for a further 1.5 hour, the solution was brought to -10 °C. 1,3-dibromopropane (0.44 mL, 4.3 mmol) was injected, and the reaction was then brought to room temperature, stirring under an inert atmosphere (Ar) for another 30 hours. A color change from dark red to dark green then to cream was observed. The reaction was quenched with water (10 mL), and the color changed to light yellow. The mixture was extracted with diethyl ether (80 mL) and dichloromethane (80 mL). The organic layer was washed with water (50 mL) and dried over anhydrous Na₂SO₄. The solvent was evaporated in a vacuum to yield an off-white powder. The crude product was purified by recrystallization from hot methanol to give a white solid. Yield: 0.89 g (51%). ¹H NMR (500 MHz, *d*-CDCl₃) δ = 8.57 (d, 4H), 8.35 (s, 4H), 7.20 (t, 4H), 2.74 (t, 4H), 2.49 (s, 6H), 1.78 (m, 4H), 1.45 ppm (m, 2H).



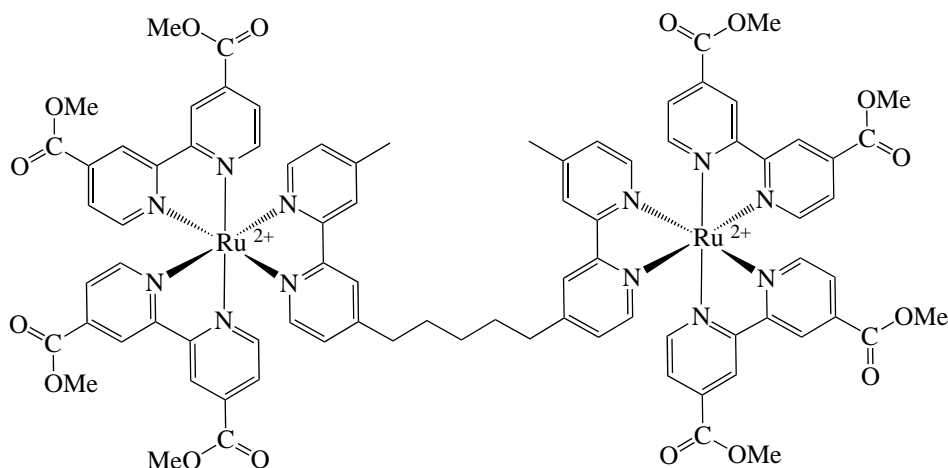
RuP-RuP (ester form), 7. The synthesis of complex **7** was based on group's previous paper.⁵ Ruthenium(II) complex **5** (206 mg, 0.20 mmol) was refluxed in 30 mL of methanol/water (1/1 v/v) under argon for 1 hour. Linker **6** (410 mg, 0.1 mmol) was dissolved in 25 mL of methanol/water and added dropwise over a period of 30 minutes. The solution was refluxed for 23 hours in the dark. The solvent was evaporated and dried overnight and purified by passage over a column of Sephadex LH-20, using methanol as the eluent (4 g packed in a column h = 30 cm, d = 20 mm). The solid was dried in oven for 2 days to give the dark red powder. ¹H NMR (500 MHz, *d*₄-MeOD): δ = 8.86 (dd, 8H), 8.57 (d, 4H), 7.89 (d, 4H), 7.83 (d, 4H), 7.68 (dd, 4H), 7.54 (dd, 4H), 7.35 (dd, 4H), 3.93 (m, 32H), 2.84 (t, 4H), 2.57 (s, 6H), 1.78 (m, 4H), 1.49 (m, 2H), 1.21 ppm (t, 48H); ³¹P NMR (202 MHz, *d*₄-MeOD): δ = 6.10 ppm (s).

RuP-RuP, 1. Hydrolysis of the phosphonate esters was accomplished based on a previous paper.⁵ To a solution of **7** (70 mg, 0.028 mmol) in 10 mL of dry DMF was added 0.66 mL (5 mmol) of bromotrimethylsilane. The mixture was heated at 60 °C under argon in the dark for 18 hours. After cooling to room temperature, the solvent was evaporated. 20 mL of MeOH was added to dissolve the residue and the solution was stirred at room temperature for 3 hours. The solvent was removed. The desired solid was red in color and used without further purification. ¹H NMR (500 MHz, *d*₂-D₂O): δ = 8.79 (dd, 8H), 8.38 (dd, 4H), 7.90 (d, 8H), 7.58 (d, 8H), 7.23 (dd, 4H), 2.79 (t, 4H), 2.47 (s, 6H), 1.71 (m, 4H), 1.40 ppm (m, 2H); ³¹P NMR (202 MHz, *d*₂-D₂O): δ = 6.86 ppm (s); MS (ESI) calculated for (C₆₇H₆₈N₁₂O₂₄P₈Ru₂)⁴⁺ 469.511, found 469.927.

General methods for the synthesis of Sensitizer 2 (RuC-RuC)



cis-[Ru(4,4'-(CO₂Me)₂bpy)₂Cl₂], 8. 4,4'-Bis(methoxycarbonyl)-2,2'-bipyridine (230 mg, 0.846 mmol), Dichlorotetrakis(dimethyl sulfoxide) ruthenium (II) (205 mg, 0.423 mmol) and LiCl (286 mg, 6.8 mmol) was dissolved in dry DMF (10 mL). The mixture was heated under reflux for 6 hours under an inert atmosphere (Ar) in the dark. After cooling to room temperature, DCM (10 mL) was added in to yield the violet red products. After being filtered and washed with DCM, the solid was dried in a vacuum and used as prepared.¹⁰

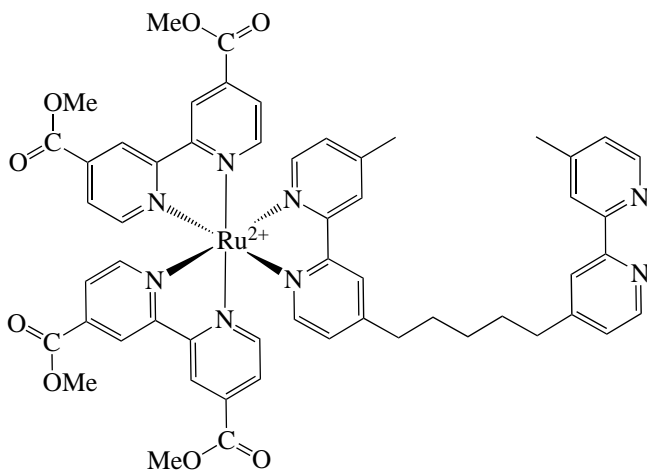


RuC-RuC (ester form), 9. Ruthenium(II) complex **8** (360 mg, 0.503 mol) was added to 30 mL of methanol/water (1:1), and the solution was refluxed for 1 hour under an inert atmosphere (Ar) in the dark. Linker **6** (103 mg, 0.252 mmol) dissolved in 25 mL of methanol/water (1:1) was added dropwise over a period of 30 minutes. The solution was under reflux in the dark for 23 hours. Upon cooling to room temperature, solvent was removed. The crude was purified over Sephadex LH-20 with methanol and dried in a vacuum overnight.⁵ ¹H NMR (500 MHz, *d*₄-MeOD): δ = 9.04 (s, 8H), 8.70 (d, 4H), 7.88 (d, 8H), 7.85 (dd, 8H), 7.63 (dd, 4H), 7.36 (dd, 4H), 3.33 (m, 24H), 2.88 (t, 4H), 2.70 (s, 6H), 1.78 (m, 4H), 1.45 ppm (m, 2H).

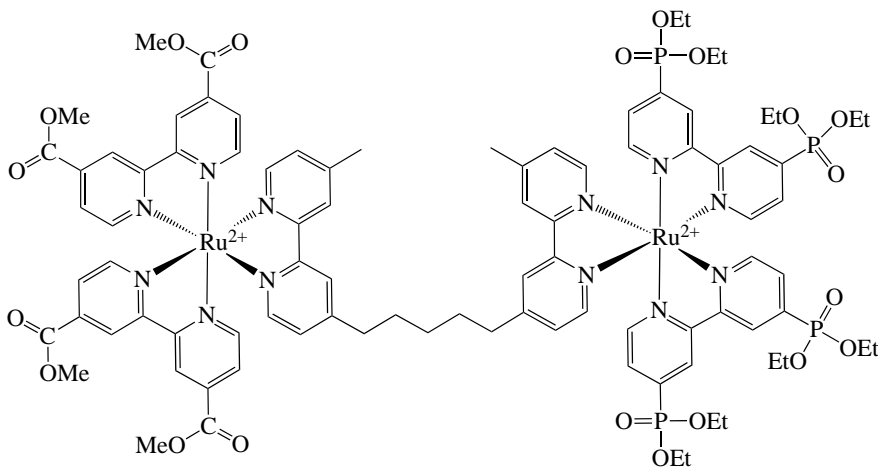
RuC-RuC, 2. HCl (6 M, 10 mL) was added to ester form **9** (50 mg). The solution was refluxed under an inert atmosphere (Ar) in the dark overnight. After cooling to the room

temperature, solvent was evaporated to afford products (56 mg, 0.032 mmol).⁵ ¹H NMR (500 MHz, *d*₄-MeOD): δ = 9.16 (s, 8H), 8.76 (d, 4H), 8.08 (d, 8H), 8.03 (dd, 8H), 7.66 (dd, 4H), 7.45 (dd, 4H), 2.90 (t, 4H), 2.62 (s, 6H), 1.84 (m, 4H), 1.54 ppm (m, 2H); MS (ESI) calculated for (C₇₅H₆₀N₁₂O₁₆Ru₂)⁴⁺ 397.558, found 397.209.

General methods for the synthesis of Sensitizer 3 (RuC-RuP).



RuC-6, 10. A solution of linker **6** (409 mg, 1 mmol) in 10 mL of methanol was firstly brought to reflux under an Ar atmosphere. A solution of **8** (358 mg, 0.5 mmol) in 50 mL of methanol was added dropwise, and the resulting solution was refluxed for 2 hours. The reaction mixture was evaporated to dryness. The crude was firstly recrystallization by methanol to remove excess **6**, followed by purified via Sephadex LH-20.¹² ¹H NMR (500 MHz, *d*₄-MeOD): δ = 8.59 (dd, 2H), 8.50 (dd, 2H), 8.12 (s, 2H), 7.89 (d, 6H), 7.84 (d, 6H), 7.60 (dd, 2H), 7.34 (dd, 4H), 3.37 (m, 12H), 2.86 (t, 2H), 2.75 (t, 2H), 2.58 (s, 3H), 2.48 (s, 3H), 1.79 (m, 4H), 1.49 (m, 2H).



RuC-RuP (ester form), 11. Ruthenium(II) complex **5** (0.22 g, 0.213 mmol) was dissolved in 50 mL of methanol/water (1:1), and the mixture was heated under reflux in an inert atmosphere (Ar) in the dark for 1 hour. Compound **10** (0.24 g, 0.213 mmol) was dissolved in 25 mL of methanol/water and added dropwise over 30 minutes. After 6-hour reflux, the solvent was evaporated and purified by passage over a column of Sephadex

LH-20, using methanol as the eluent (4 g packed in a column h = 30 cm, d = 20 mm).⁵ ¹H NMR (500 MHz, *d*₄-MeOD): δ = 9.18 (s, 8H), 8.73 (d, 2H), 8.71 (d, 2H), 8.05 (d, 8H), 7.97 (dd, 8H), 7.64 (dd, 4H), 7.37 (dd, 4H), 4.10 (m, 12H), 3.69 (m, 16H), 2.92 (t, 4H), 2.56 (s, 6H), 1.83 (m, 4H), 1.53 (m, 2H), 1.30 (t, 24H); ³¹P NMR (202 MHz, *d*₄-MeOD): δ = 8.55 ppm (s).

RuC-RuP, 3. HCl (6 M, 10 mL) was added to **11** (119 mg) in the ester form. The solution was refluxed at 100 °C under an inert atmosphere (Ar) in the dark overnight. After cooling to the room temperature, the solvent was evaporated to afford a product. ¹H NMR (500 MHz, *d*₄-MeOD): δ = 9.18 (s, 8H), 8.73 (d, 2H), 8.71 (d, 2H), 8.05 (d, 8H), 7.97 (dd, 8H), 7.64 (dd, 4H), 7.37 (dd, 4H), 2.90 (t, 4H), 2.63 (s, 6H), 1.81 (m, 4H), 1.55 ppm (m, 2H); ³¹P NMR (202 MHz, *d*₄-MeOD): δ = 8.05 ppm (s); MS (ESI) calculated for (C₇₁H₅₈N₁₂O₂₀P₄Ru₂) [M-6H]²⁻ 864.047, found 863.745.

Photoanode Preparation

Anatase TiO₂ nanoparticle electrodes were prepared on a fluorine-doped glass (FTO) plate. A colloidal suspension of TiO₂ prepared previously was deposited onto the FTO glass (1 cm² area) through the doctor blade method.⁸ The prepared TiO₂-coated electrodes were calcined at 300 °C for 20 minutes, 350 °C for 10 minutes, and 500 °C for 30 minutes. After cooling to room temperature, electrodes were sensitized by soaking in 0.1 mM solution of each sensitizer in the dark for 24 hours to allow the full adsorption of the molecular sensitizer. Sensitizers **2** (RuC-RuC) and **3** (RuC-RuP) were dissolved in methanol; sensitizer **1** (RuP-RuP) was dissolved in a mixture of methanol, water and 0.1 M HCl. It was found that the solubility profiles of the three complexes were different. Generally, the increasing number of phosphonate groups decreased the solubility of the complex in methanol. All electrodes were kept in the dark before use.

Photostability Measurements

The photostability of the sensitizers was measured by putting the electrodes under constant irradiation (10 mW/cm²). The light from a royal blue LED with a nominal wavelength of 455 nm and a bandwidth of 18 nm was directed onto the sensitized electrodes. Prepared electrodes were placed in the acetate buffer (pH 4.9) or potassium phosphate buffer (pH 6.9) and illuminated with constant irradiation (10 mW/cm²) for 2 hours. The absorbance of the electrodes was measured to determine the amount of molecular sensitizer adsorbed on the electrode surface. Data were collected every 5 minutes over the first 30 minutes, every 10 minutes over another 30 minutes and every 20 minutes throughout another hour. The electrodes were rinsed with methanol between each measurement and dried under a stream of N₂.

Geometry Optimization from Density Functional Theory (DFT) Calculations

A preliminary study on the binding mode between the sensitizer and TiO₂ surface was conducted by using the density functional theory (DFT) approach in Gaussian 16 program package. The position of the anchoring groups in the bipyridine ligands in relation to the metal center can generate different geometric isomers. In the calculations, four geometric isomers of complex **1** were drawn as the initial structures. The geometry optimization of those isomers was calculated by B3LYP functional and 6-31G basis sets

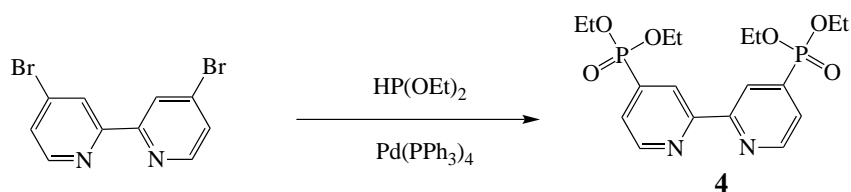
for all the atoms except Ru. For Ru, the LANL2DZ was adopted. The geometries were optimized in the gas phase with no counterions to balance charges. The calculation was carried out for each structure and the positive frequencies were taken into consideration as an indication for completed optimization. The energy obtained for each of the different isomers was compared and the structure with the lowest energy was selected as an optimized final geometry.

Results and Discussion

Synthesis

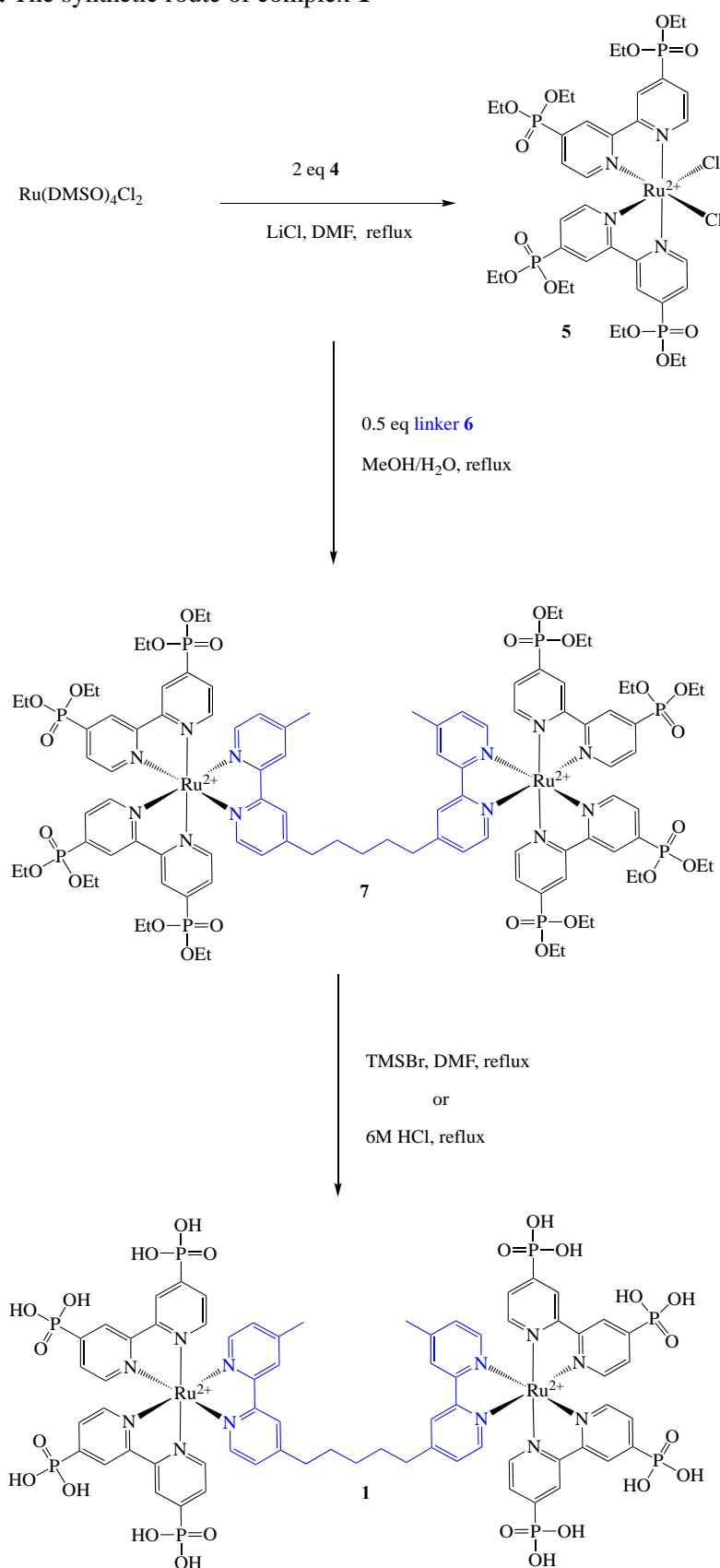
Two types of anchors are synthesized in this study. They differ in the substitution (carboxylate or phosphonate) at the 4,4' positions of bipyridine ligands. The phosphonate ester anchor **4** (**Scheme 1**) can be prepared by palladium cross coupling of diethylphosphite with the corresponding dibromo bipyridine.⁹ This reaction is widely used to synthesize bipyridine phosphonate ligands and gives high yields. The carboxylate anchors are widely commercially available in the ester form, and a one-step hydrolysis of the ester gives the acid.

Scheme 1. The synthetic route of diphosphonate ester bipyridine ligand **4**

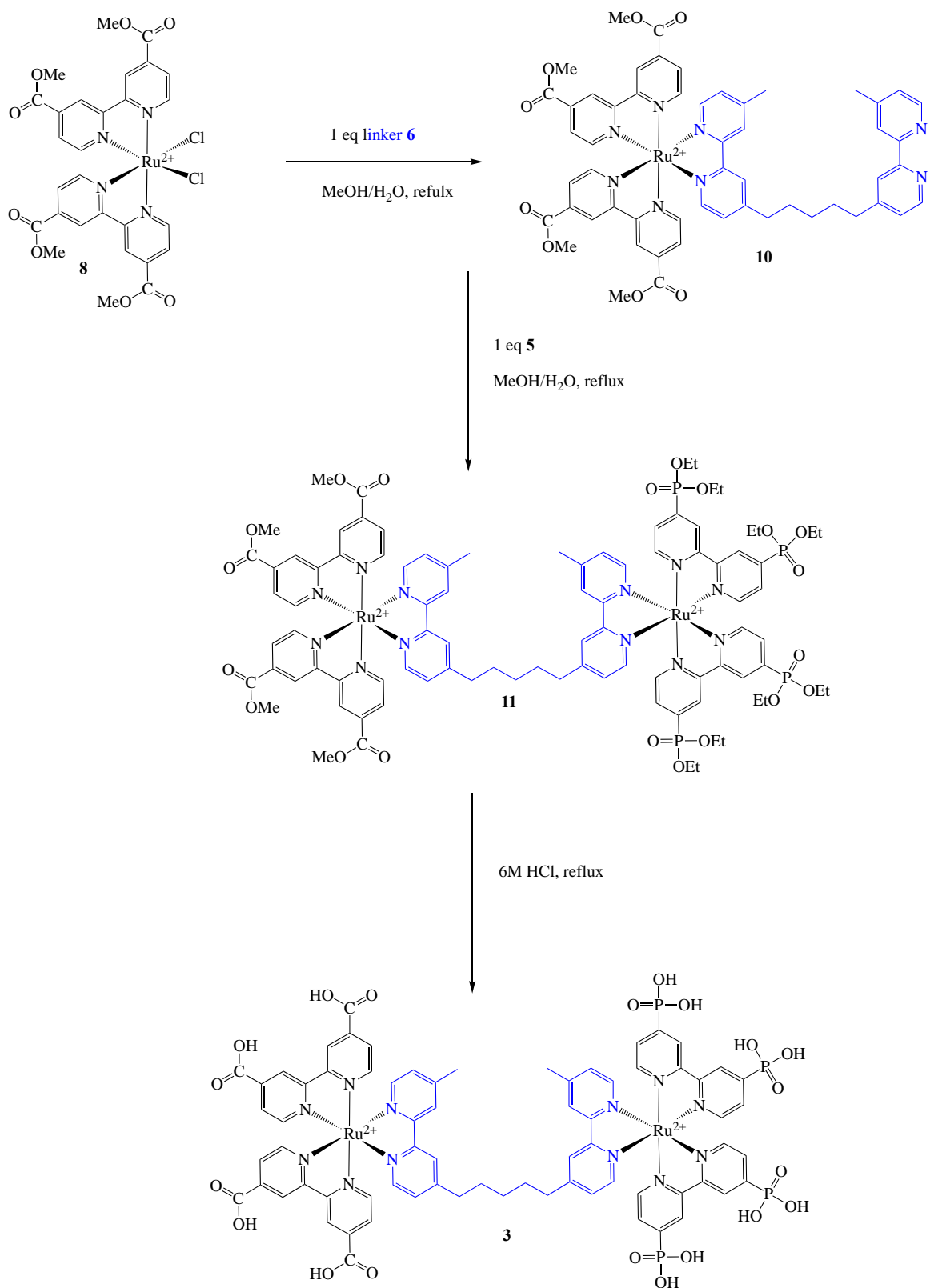


To probe the influence of variations in the identity of anchor, three ruthenium(II) complexes (**1**, **2** and **3**) are synthesized. Due to the symmetric structure of the complex, the outer unit **5** is synthesized first, then coupled with the inner linker **6** (in blue color) to achieve the target structure. An approach to synthesize **1** is shown in **Scheme 2**. The first step is accomplished by treating *tetrakis*(dimethylsulfoxide)ruthenium(II) chloride with 2 equivalents of the bipyridine ligand **4**. The product **5** is red-orange in color. Coupling 2 equivalents of the outer unit **5** and 1 equivalent of linker **6** (shown in blue in Scheme 2), sensitizer **1** in the ester form (**7**) is obtained. During the reaction, the phosphonate ester groups are partly hydrolyzed. Complex **7** is purified by size exclusion chromatography using Sephadex LH-20 before the next step. Full hydrolysis of the phosphonate esters can be accomplished either by refluxing in hydrochloric acid or by adding bromotrimethylsilane in dimethylformamide.⁷ Using the same synthetic protocol, the sensitizer **2** can be produced. The synthetic route to complex **3** (**Scheme 3**) has more steps than the synthesis of **1** and **2** due to the unsymmetric structure. The first step is to couple linker **4** with complex **8** to yield **10**. In this procedure, a solution of **8** in methanol is added dropwise to a solution of **4** to give **10**. Unlike the hydrolysis of **7**, which can be achieved by two routes, complex **11** has a poor solubility in DMF. Therefore, hydrochloric acid is used to hydrolyze **11**, and complex **3** is obtained as a dark red solid.

Scheme 2. The synthetic route of complex **1**



Scheme 3. The synthetic route of complex **3**



Photostability Measurements

The stability of anchoring groups in aqueous media is generally regarded as the most important factors to consider when designing WS-DSPECs. The choice of anchoring group should be primarily based on the operating conditions to be employed. A key factor is pH because the various anchoring groups have different pH stability ranges when anchored to metal oxide surfaces. A visual change in the color of the electrodes is observed during the measurements. A photograph of an electrode (sensitizer **2**) before and after irradiation at pH 4.9 (**Figure 3**) is shown as an example. The color of the electrodes becomes lighter after operation for two hours indicates the decreasing amount of binding sensitizers. Therefore, a quantitative study of the desorption is performed.

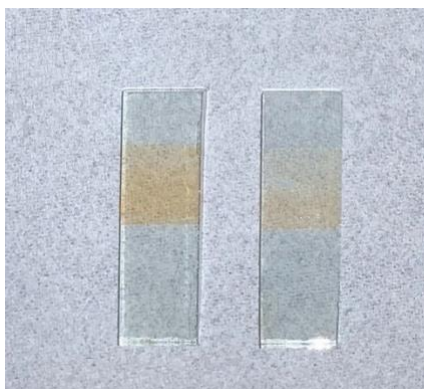


Figure 3. A photograph of electrode (sensitizer **2**) before and after desorption at pH 4.9

Anchoring group stability is typically characterized through UV-Vis spectroscopic monitoring in surface desorption experiments.⁴⁻⁷ **Table 2** lists the absorption band positions obtained from UV-Vis spectra. The three sensitizers exhibit metal-to ligand charge transfer (MLCT, $d \rightarrow \pi^*$) bands in the visible region *ca.* 460 nm, consistent with values found in the literature.¹³ Ruthenium (II) polypyridyl derivatives with similar MLCT absorptions are widely used as molecular sensitizers in WS-DSPECs.⁴⁻⁸ Thus, the results from this study indicate that compounds **1**, **2** and **3** should be suitable for constructing the desired photoelectrochemical cells.

Table 2. MLCT band positions of molecular sensitizers

Ruthenium Sensitizers	λ_{\max} (nm)
RuP-RuP 1	460
RuC-RuC 2	465
RuC-RuP 3	458

The UV-Vis absorption spectra of the three molecular sensitizers on TiO₂ are monitored both before and after desorption. The Beer-Lambert Law, Equation 1, is the principle behind absorbance spectroscopy. A is absorbance (unitless), ϵ is the molar absorptivity of the compound ($M^{-1}cm^{-1}$), b is the path length of the cuvette or sample holder (cm), and c is the concentration of the species (M).

$$A = \epsilon bc \quad (1)$$

For each sensitizer, the path length of the cuvette and the molar absorptivity can be assumed as the same. There is a linear relationship between the concentration and the absorbance of the solution, which enables the concentration to be calculated by measuring its absorbance. According to other groups' study, there are no spectral changes for an electrode of sensitizers on TiO₂ surface in aqueous solvent in the dark over a long period.¹⁵ Therefore, the amount of adsorption of each sensitizer on TiO₂ can be estimated by comparison of the concentrations before and after the irradiation. A larger difference in intensity indicates a large amount of desorption from the electrode, suggesting a poorer photostability of the sensitizer. In addition, the performance of the anchoring group is primarily based on the operating. A key factor is pH because the various anchoring groups have different pH stability ranges when binding to metal oxide surfaces. The acetate buffer (pH 4.9) and the potassium phosphate buffer (pH 6.9) are used as the operating conditions for the photostability measurements in this study. Results for each sensitizer are displayed in **Figure 4** and **Figure 5**.

Dye-sensitized electrodes are placed in the acetate buffer (pH 4.9) and illuminated with constant irradiation (10 mW/cm^2) under irradiation for 2 hours. Absorption spectra are displayed in **Figure 4**. The absorption values are normalized at the absorption maxima from **Table 2**. The MLCT feature decreases in intensity (the plotting color in each figure changes from dark to light with increasing time) for the three sensitizers due to the desorption of complexes from TiO₂ surface under light irradiation. Specifically, the absorbance decreases from 1 to ~ 0.85 for sensitizer **1** with phosphonate anchors (**Figure 4a**). Changing the phosphonate groups to carboxylate, a more obvious absorbance change is observed. Complex **2** (**Figure 4b**) with carboxylate anchors shows a ~ 0.55 drop in absorbance, while complex **3** (**Figure 4c**) with both carboxylate and phosphonate anchors drops to ~ 0.7 after operation. Changes in absorbance over time during desorption experiments for three sensitizers are shown in **Figure 4d**. Sensitizer **1**, **2**, and **3** are plotted in black, red and orange respectively. The MLCT absorbance of **2**-sensitized electrodes decreased the most rapidly as a result of desorption, followed by sensitizer **3**. sensitizer **1** exhibits a minimal change in absorbance among three complexes. Generally, the three sensitizers show a final absorbance in the ratio of 85:70:55 after 2-hour irradiation. A lower MLCT feature indicates a weaker light absorbing ability and reflects a less photostability. Therefore, complexes **1** (RuP-RuP) and **3** (RuC-RuP) adsorb more persistently on the TiO₂ electrodes compared with **2** (RuC-RuC). The results illustrate that the phosphonate anchor can enhance the photostability of sensitizers compared to the carboxylate at pH 4.9.

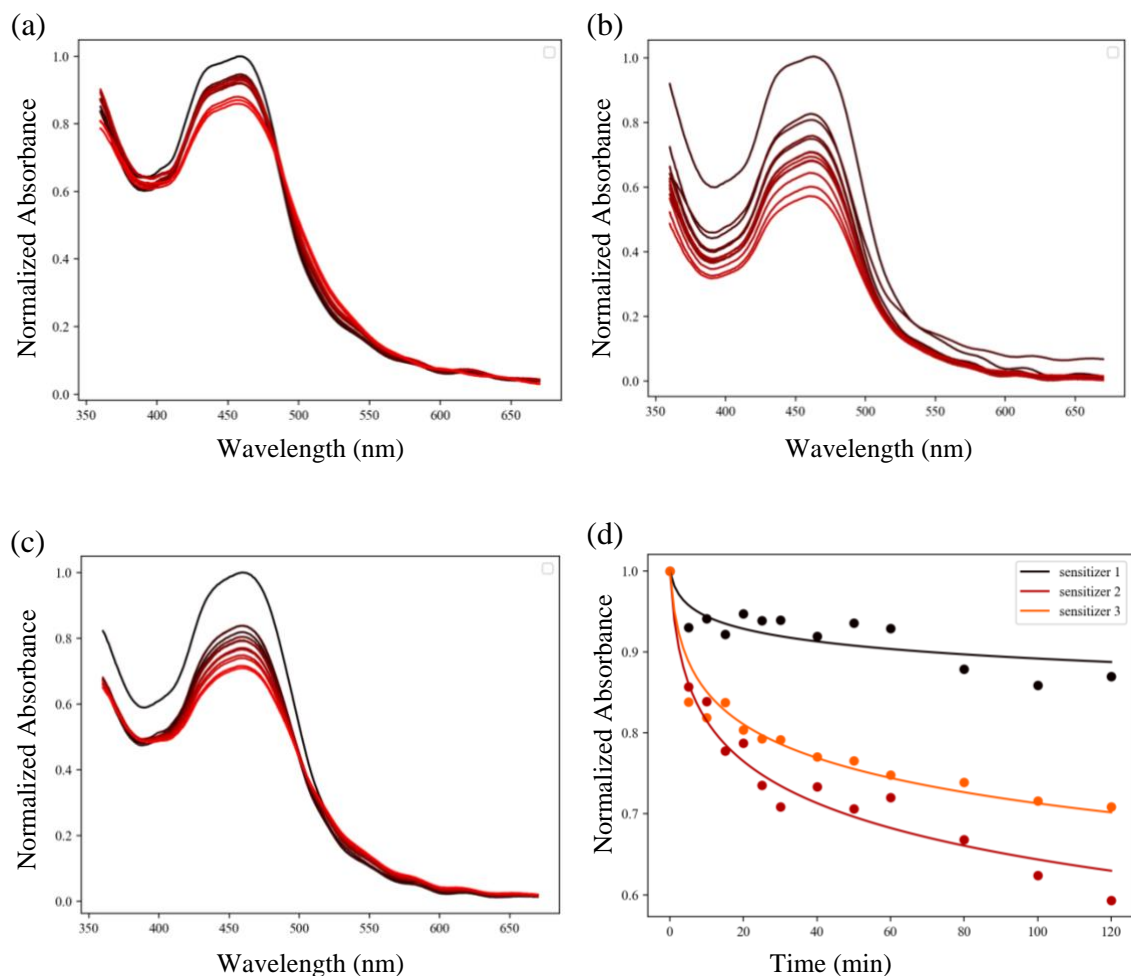


Figure 4. Absorbance of sensitizers at pH 4.9. The UV-Vis spectra are normalized at the absorption maxima. The data are collected every 5 minutes over the first 30 minutes, every 10 minutes over another 30 minutes and every 20 minutes throughout the rest 1 hour. (a) Sensitizer 1 RuP-RuP, (b) Sensitizer 2 RuC-RuC, (c) Sensitizer 3 RuC-RuP, (d) Changes in absorbance over time during desorption experiments at pH 4.9.

While all complexes are found to bind to electrodes effectively under acidic conditions (pH 4.9), the sensitizers exhibit lower photostability on changing the pH to neutral (pH 6.9). Dye-sensitized electrodes are placed in the potassium phosphate buffer (pH 6.9) and illuminated with constant irradiation (10 mW/cm^2). The data in **Figure 5** are collected for 30 minutes. Sensitizer 1 (**Figure 5a**) and sensitizer 3 (**Figure 5c**) show absorbance decreases from 1 to ~ 0.15 , and 1 shows a slower rate of MLCT absorption loss. Sensitizer 2 (**Figure 5b**) shows facile desorption from the electrode under these conditions, and the MLCT band reaches the baseline after 5 minutes of irradiation. Changes in absorbance versus time during desorption at pH 6.9 for three sensitizers are illustrate in **Figure 5d**, and trends for the absorbance change are more obviously observed. Sensitizer 1, 2, and 3 are plotted in black, red and orange respectively. By the end of the 30 minutes experiment, the sensitizer 2 desorbs from the surface completely, and the absorbance reaches zero. Generally, the three sensitizers show a final absorbance in the ratio of

85:85:0 after 30-minute irradiation. Because a smaller intensity drop illustrates a stronger photostability, sensitizer **1** with the phosphonate anchors provides the persistent adsorbing at pH 6.9 under constant irradiation (10 mW/cm^2). These results are in agreement with data collected under acidic conditions, that the phosphonate groups can enhance the photostability of sensitizers on TiO_2 surfaces compared with carboxylate groups at pH 6.9.

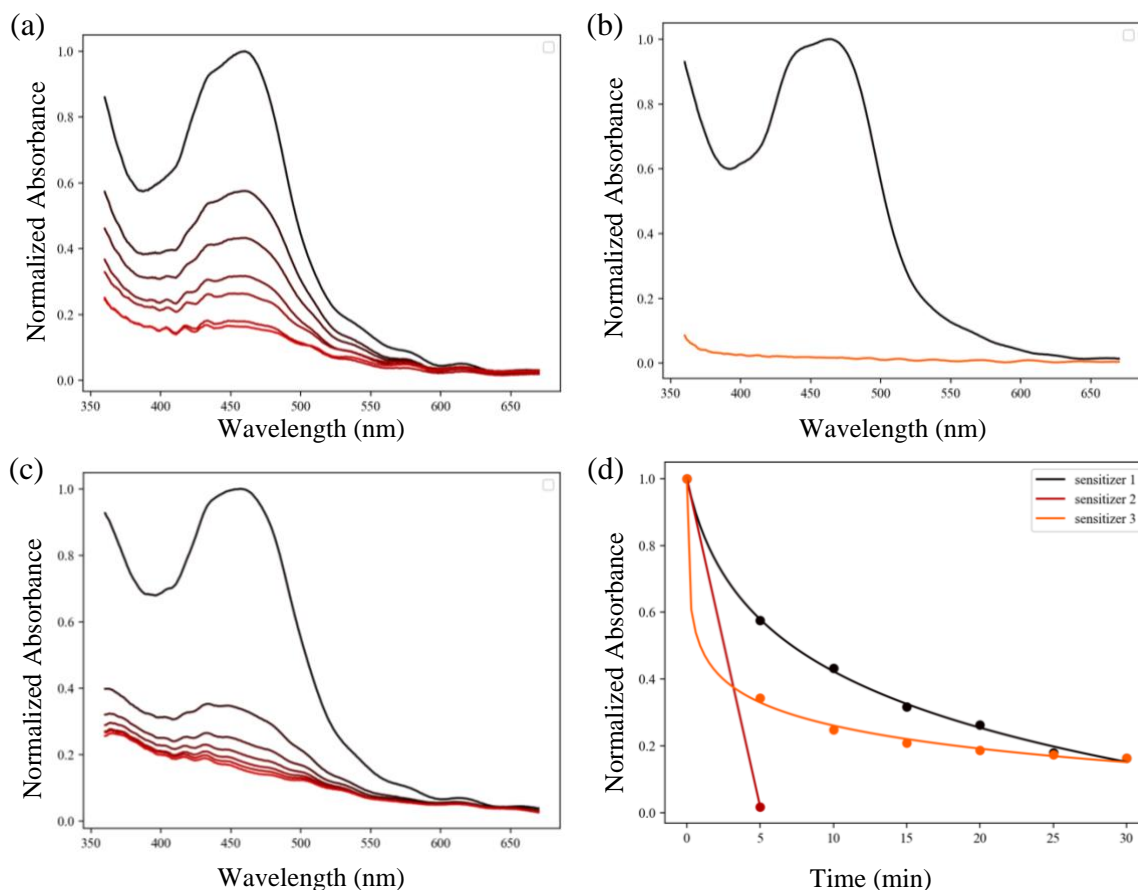


Figure 5. Absorbance of sensitizers at pH 6.9. The UV-Vis spectra are normalized at the absorption maxima. The data are collected every 5 minutes over 30 minutes. (a) Sensitizer **1** RuP-RuP, (b) Sensitizer **2** RuC-RuC, (c) Sensitizer **3** RuC-RuP, (d) Changes in absorbance over time during desorption experiments pH 6.9.

Overall, substantial desorption of the sensitizers is observed at neutral pH; in contrast, sensitizers have smaller changes in absorbance at acidic solution. The data collected in **Figure 4** and **Figure 5** indicate that the sensitizer with the phosphonate anchors can effectively adsorb on the TiO_2 surface at pH from 4.9 to 6.9, while the carboxylate substituted sensitizer only gives a moderate stability at low pH (< 4.9). Similar trends for the photostability are obtained from other groups as well.^{6,13} Those studies find that the surface binding (strength and stability) of sensitizers on TiO_2 is highly influenced by the

number of carboxylate and phosphonate groups and is a decisive factor in controlling the sensitization efficiency. According to Nilsing's theoretical study, the adsorption energy for phosphonate anchors is almost twice as large as the carboxylate group, and phosphonate groups are found to bind substantially more strongly to the anatase surface.¹⁴ According to Park's study, the attraction between the carboxylate groups and the TiO₂ surface prevails at pH < 4, while adsorption of the phosphonate groups on TiO₂ is highly efficient up to pH 7. Trends for the stability are almost consistent with this study. Results from the photostability measurements broaden the pH range at which WS-DSPECs can be studied by substituting the identity of the anchor. Implications for the design of the sensitizers in WS-DSPECs can be learnt. The non-aqueous solvent solubility of sensitizers is an important factor to consider when designing new molecules for the cell. As mentioned above, the sensitizer **1** with the phosphonate anchors has poor solubility in non-aqueous solvents like methanol, requiring the use of water as the main solvent to dissolve the material. Proton intercalation is known to occur in solutions with very dilute proton concentrations, and the surface trap states are formed on TiO₂ electrodes.¹⁶ This intercalation can work to reduce the injection yield, which will be measured later in this project. Although phosphonate groups can largely enhance the binding affinity, their insolubility in desired solvents like methanol is a serious issue to influence electron-transfer dynamics of sensitizers.

Geometry Optimization of Sensitizer **1**

A preliminary study on the binding mode between the sensitizer and TiO₂ surface was conducted by using the density functional theory (DFT) approach. The position of the anchoring groups in the bipyridine ligands in relation to the metal center can generate different geometric isomers. These isomers determine the binding properties to the TiO₂ surface. The calculations were completed in gas phase and with no counterions to balance the charges. In the calculations, four geometric isomers of complex **1** were studied and the results compared to identify the structure with the lowest energy. According to the calculation, the isomer with all anchoring groups on the bipyridine ligands in *cis* positions was selected as an optimized final geometry due to the lowest energy among four initial structures. Shown in **Figure 6**, the electrostatic force between two ruthenium (II) ions results the extended conformation of the five-carbon chain. The repulsion between two metal centers was due to lack of counterions to balance charges. Subsequent calculations will probe the effect of including counterions in the geometry optimization.

Previous work shows that the sensitizers are typically bound to the TiO₂ surface through oxygen-containing substituents (shown in red and orange in **Figure 6**),¹⁴ It is hypothesized that the strength of the interaction between the sensitizer and the electrode surface are one of the most important factors to determine the photostability. The experimental results illustrate that sensitizer **1** has the largest number of phosphonate anchors and exhibits the best photostability at pH from 4.9 to 6.9. In order to test this hypothesis, similar computational studies will be completed with synthesizers **1**, **2** and **3**. The results will help understand the binding mode of the optimized geometries to the TiO₂ surface. The binding strength will be compared and to support the experimental data.

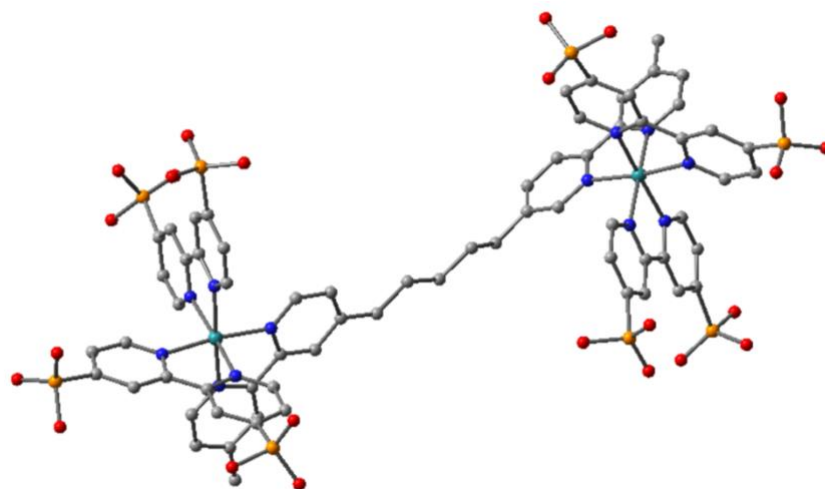


Figure 6. The optimized geometrical structure of sensitizer **1**. H is omitted for clarity. Color coding: C—grey, O—red, N—blue, P—orange, Ru—cyan.

Conclusion and Future Work

In summary, the ruthenium(II) sensitizers **1**, **2** and **3** are obtained and characterized. Sensitizer **1**, which contained the highest number of phosphonate groups, shows the best photostability among three sensitizers over pH ranges from 4.9 to 6.9. One of the major limitations of WS-DSPECs – dye desorption – is studied in this project. Incorporation of different types of anchoring groups opens up opportunities for producing more efficient sensitizers. Carboxylate and phosphonate anchoring groups have been considered widely⁴⁻⁷ for use in photoanodes for light-driven water oxidation. This study confirms that the presence of phosphonate anchors enhances the photostability of sensitizers on TiO₂ electrodes than the carboxylate at pH from 4.9 to 6.9 under the 10 mW/cm² irradiation. Trends for the anchoring stability are in agreement with others' studies.^{6,13,14}

Future work will include measuring the photoinjection yield of three ruthenium (II) sensitizers from the excited state of the sensitizer to the TiO₂ conduction band, as this is another key factor that influences the efficiency of WS-DSPECs. The previous study has confirmed that the different nature of anchoring groups (carboxylate or phosphonate groups) on the bipyridine ligands could affect the photoinjection yield in the cell.⁶ Therefore, comparing this property for **1**, **2** and **3** can give a determination of the overall performance. In addition, work will not only be confined to dinuclear complexes. The results from this report serve as a starting point for modifying oligomeric sensitizers. Trinuclear, tetranuclear, and oligomeric sensitizers with longer chain lengths might be developed using the same synthetic protocol in the future. Apart from the experimental studies, the density functional theory (DFT) approach will be focused to investigate absorption manners of sensitizers anchored to TiO₂ surface. Through the theoretical studies, how the number of anchors (through phosphonate or carboxylate groups) on the sensitizers affects the binding stability on TiO₂ will be illustrated to further support the experimental data. In terms of the application, the findings from this project can be used to separate the mixture of chemical substances. Complexes with diverse anchoring groups show different photostability properties bind to metal dioxide surface, and the desorption of complexes are primarily based on operating pH. This technique can be applied to separate mixtures with different binding stability that the component with a poor stability will desorb from surface in a high rate.

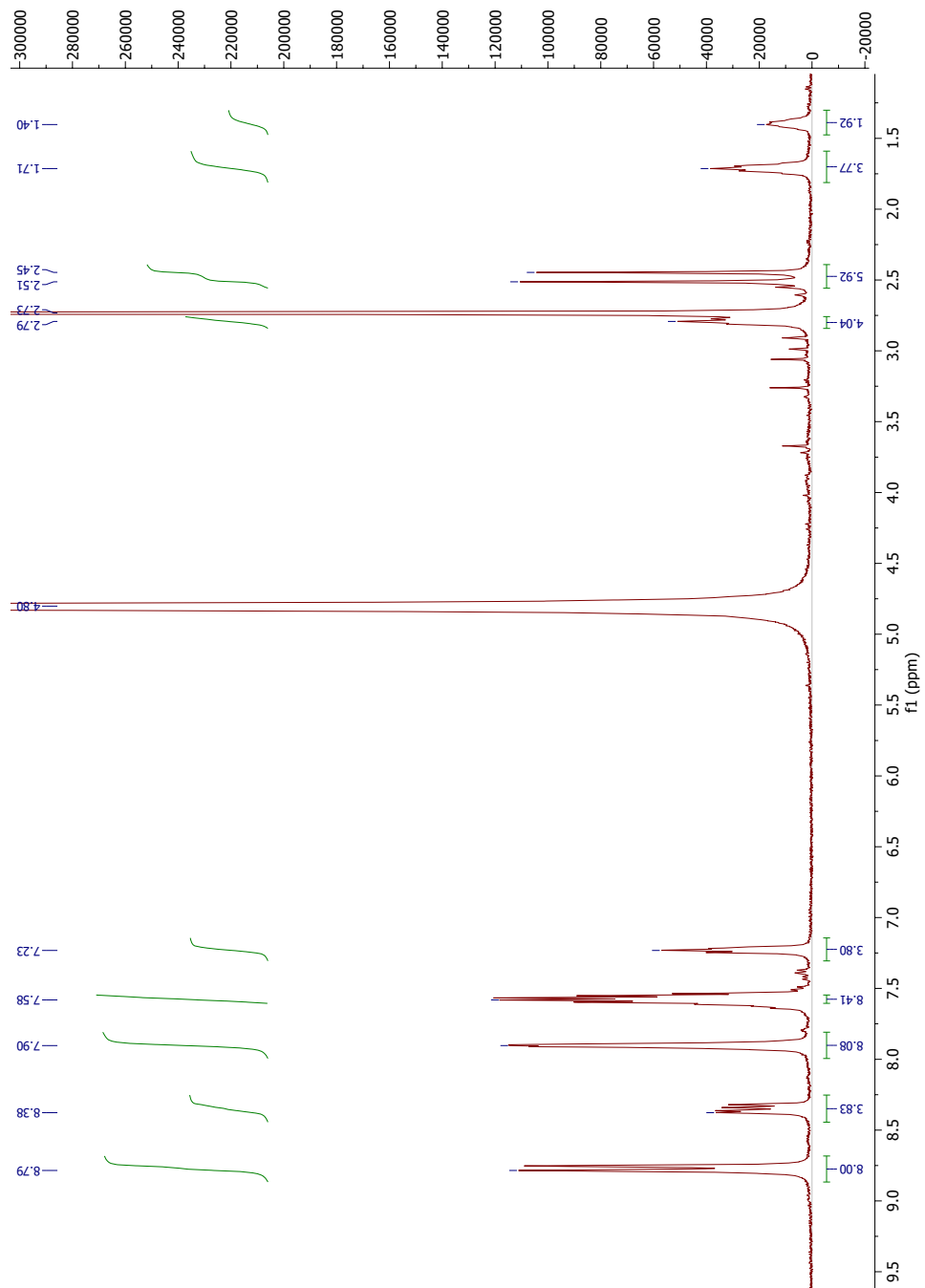
References

1. Sun, Z.; Ma, T.; Tao, H.; Fan, Q.; Han, B. Fundamentals and challenges of electrochemical CO₂ reduction using two-dimensional materials. *Chem.* **2017**, *3*, 560-587.
2. Davis, S.J.; Caldeira, K.; Matthews, H.D. Future CO₂ emissions and climate change from existing energy infrastructure. *Science* **2010**, *329*, 1330–1333.
3. Shi, J.; Jiang, Y.; Jiang, Z.; Wang, X.; Wang, X.; Zhang, S.; Han, P.; Yang, C. Enzymatic conversion of carbon dioxide. *Chem. Soc. Rev.* **2015**, *44*, 5981–6000.
4. Swierk, J.R.; Mallouk, T.E. Design and development of photoanodes for water-splitting dye-sensitized photoelectrochemical cells. *Chemical Society Reviews* **2013**, *42*, 2357-2387.
5. Gray, C.L.; Xu, P.; Rothenberger, A.J.; Koehler, S.J.; Elacqua, E.; Milosavljevic, B.H.; Mallouk, T.E. An Oligomeric Ruthenium Polypyridyl Dye for Improved Stability of Aqueous Photoelectrochemical Cells. *The Journal of Physical Chemistry C* **2020**, *124*, 3542-3550.
6. Materna, K.L.; Crabtree, R.H.; Brudvig, G.W. Anchoring groups for photocatalytic water oxidation on metal oxide surfaces. *Chemical Society Reviews* **2017**, *46*, 6099-6110.
7. Gillaizeau-Gauthier, I.; Odobel, F.; Alebbi, M.; Argazzi, R.; Costa, E.; Bignozzi, C.A.; Qu, P.; Meyer, G.J. Phosphonate-based bipyridine dyes for stable photovoltaic devices. *Inorg. Chem.* **2001**, *40*, 6073-6079.
8. Xiao, L.; Yu, Y.; Schultz, E.L.; Stach, E.A.; Mallouk, T.E. Electron Transport in Dye-Sensitized TiO₂ Nanowire Arrays in Contact with Aqueous Electrolytes. *The Journal of Physical Chemistry C* **2020**, *124*, 22003-22010.
9. Neuthe, K.; Bittner, F.; Stiemke, F.; Ziem, B.; Du, J.; Zellner, M.; Wark, M.; Schubert, T.; Haag, R. Phosphonic acid anchored ruthenium complexes for ZnO-based dye-sensitized solar cells. *Dyes and Pigments* **2014**, *104*, 24-33.
10. Zabri, H.; Gillaizeau, I.; Bignozzi, C.A.; Caramori, S.; Charlot, M.F.; Cano-Boquera, J.; Odobel, F. Synthesis and comprehensive characterizations of new cis-RuL₂X₂ (X= Cl, CN, and NCS) sensitizers for nanocrystalline TiO₂ solar cell using bis-phosphonated bipyridine ligands (L). *Inorganic chemistry* **2003**, *42*, 6655-6666.
11. Mulyana, Y.; Weber, D.K.; Buck, D.P.; Motti, C.A.; Collins, J.G.; Keene, F.R. Oligonuclear polypyridylruthenium (II) complexes incorporating flexible polar and non-polar bridges: synthesis, DNA-binding and cytotoxicity. *Dalton Transactions* **2011**, *40*, 1510-1523.
12. Wacholtz, W. F.; Auerbach, R. A.; Schmechl, R. H. Preparation, characterization, and photophysical properties of covalently linked binuclear and tetranuclear ruthenium bipyridyl complexes. *Inorganic chemistry* **1987**, *26*, 2989-2994.
13. Park, H.; Bae, E.; Lee, J.J.; Park, J.; Choi, W. Effect of the anchoring Group in Ru– Bipyridyl sensitizers on the Photoelectrochemical behavior of dye-sensitized TiO₂ electrodes: carboxylate versus Phosphonate linkages. *The Journal of Physical Chemistry B.* **2006**, *110*, 8740-8749.

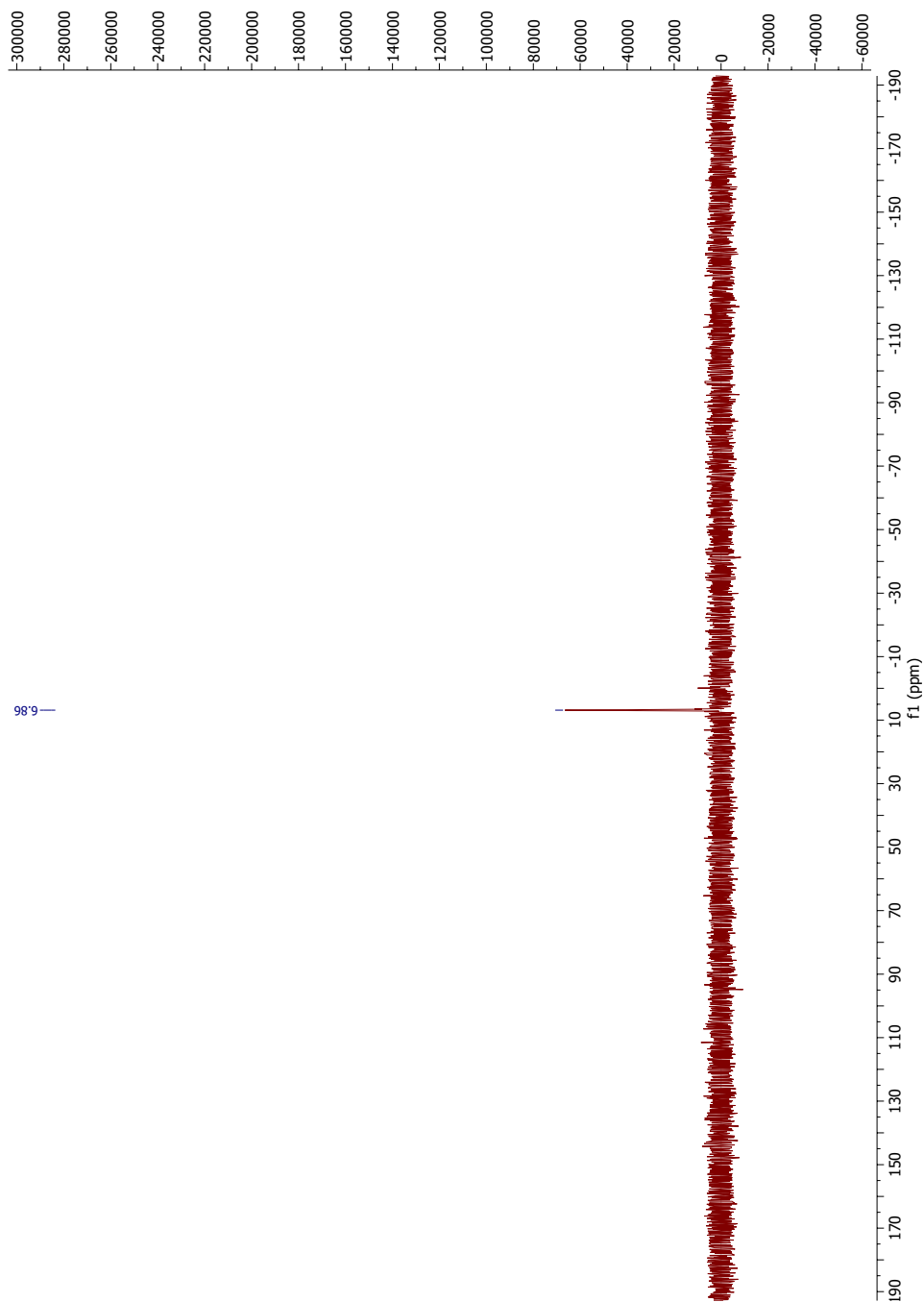
14. Nilsing, M.; Persson, P.; Ojamäe, L. Anchor group influence on molecule–metal oxide interfaces: periodic hybrid DFT study of pyridine bound to TiO₂ via carboxylic and phosphonic acid. *Chemical physics letters* **2005**, *415*, 375-380.
15. Hanson, K.; Brennaman, M.K.; Luo, H.; Glasson, C.R.; Concepcion, J.J.; Song, W.; Meyer, T.J. Photostability of phosphonate-derivatized, RuII polypyridyl complexes on metal oxide surfaces. *ACS applied materials & interfaces* **2012**, *4*, 1462-1469.
16. McCool, N.S.; Swierk, J.R.; Nemes, C.T.; Saunders, T.P.; Schmittenmaer, C.A.; Mallouk, T.E. Proton-induced trap states, injection and recombination dynamics in water-splitting dye-sensitized photoelectrochemical cells. *ACS applied materials & interfaces* **2016**, *8*, 16727-16735.

Appendices

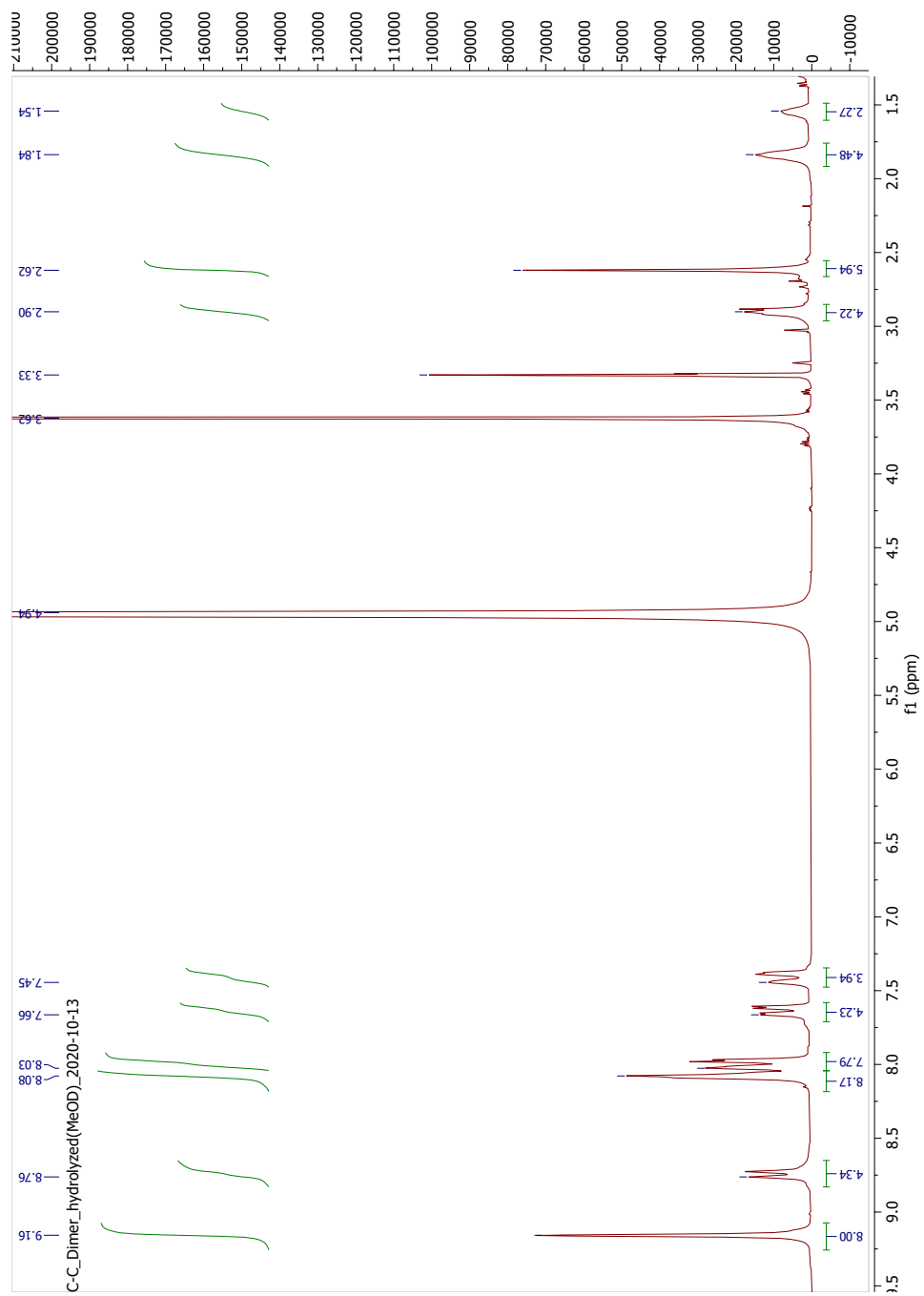
Appendix 1. ^1H NMR of **1**



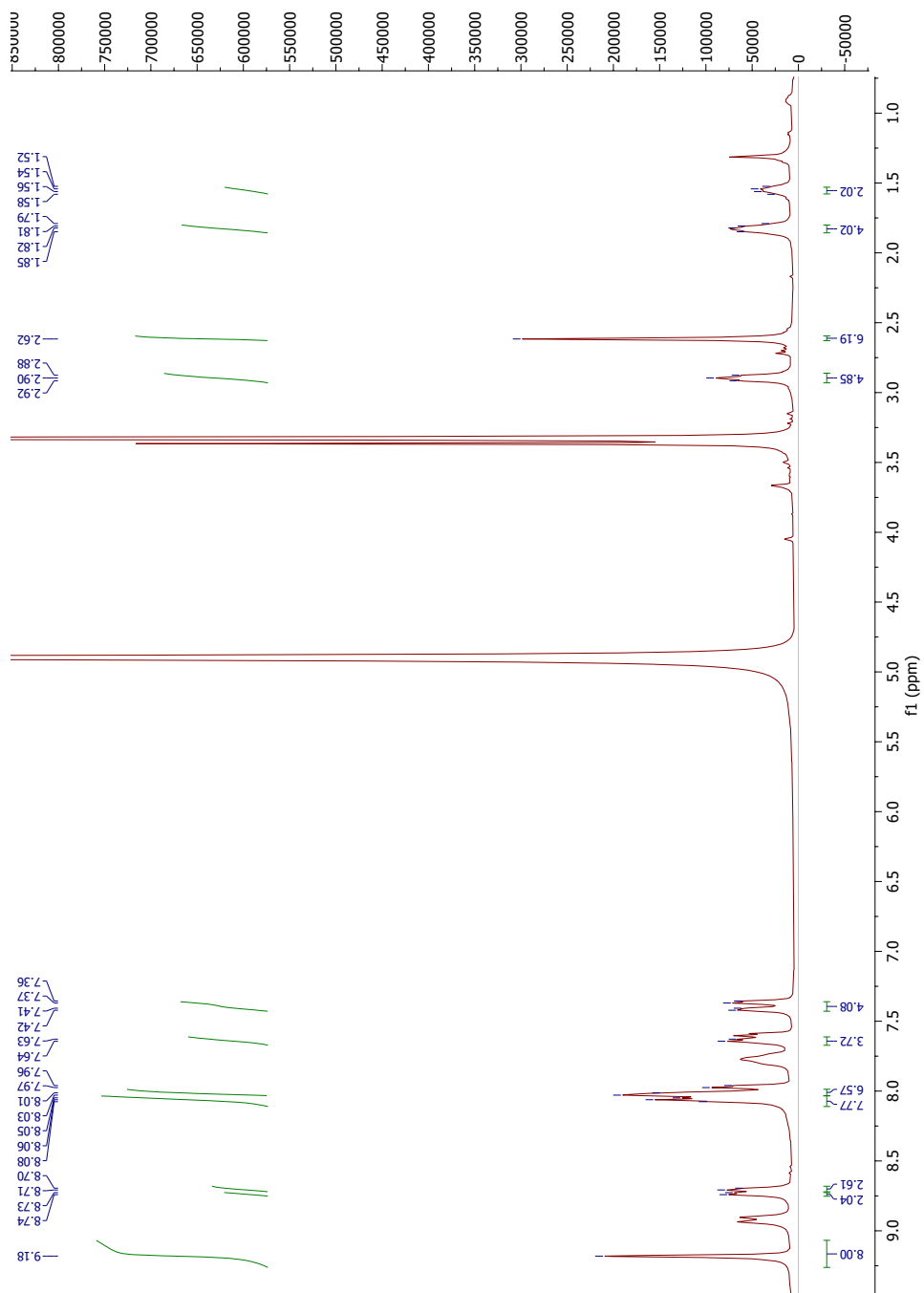
Appendix 2. ^{31}P NMR of 1



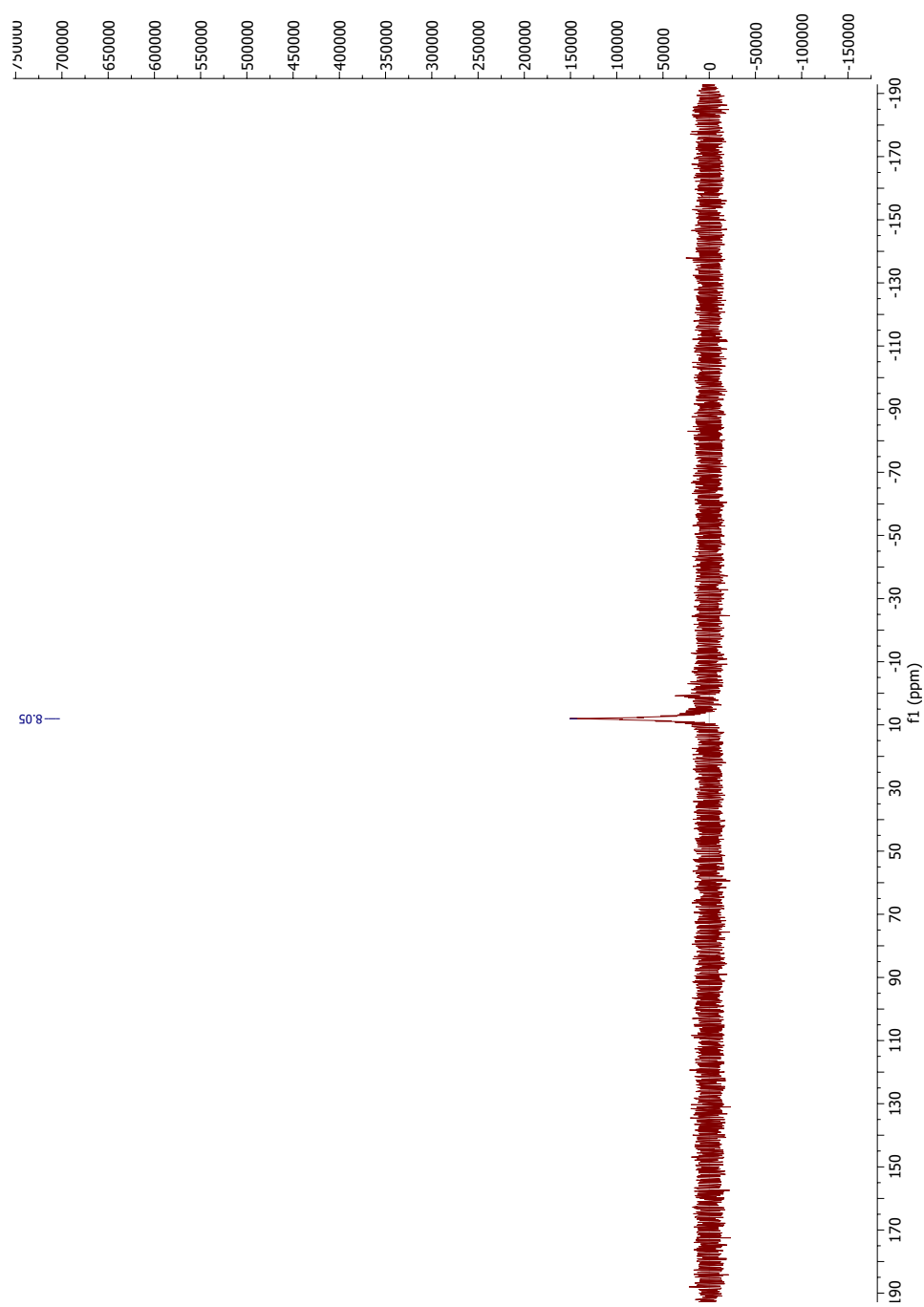
Appendix 3. ^1H NMR of 2



Appendix 4. ¹H NMR of 3

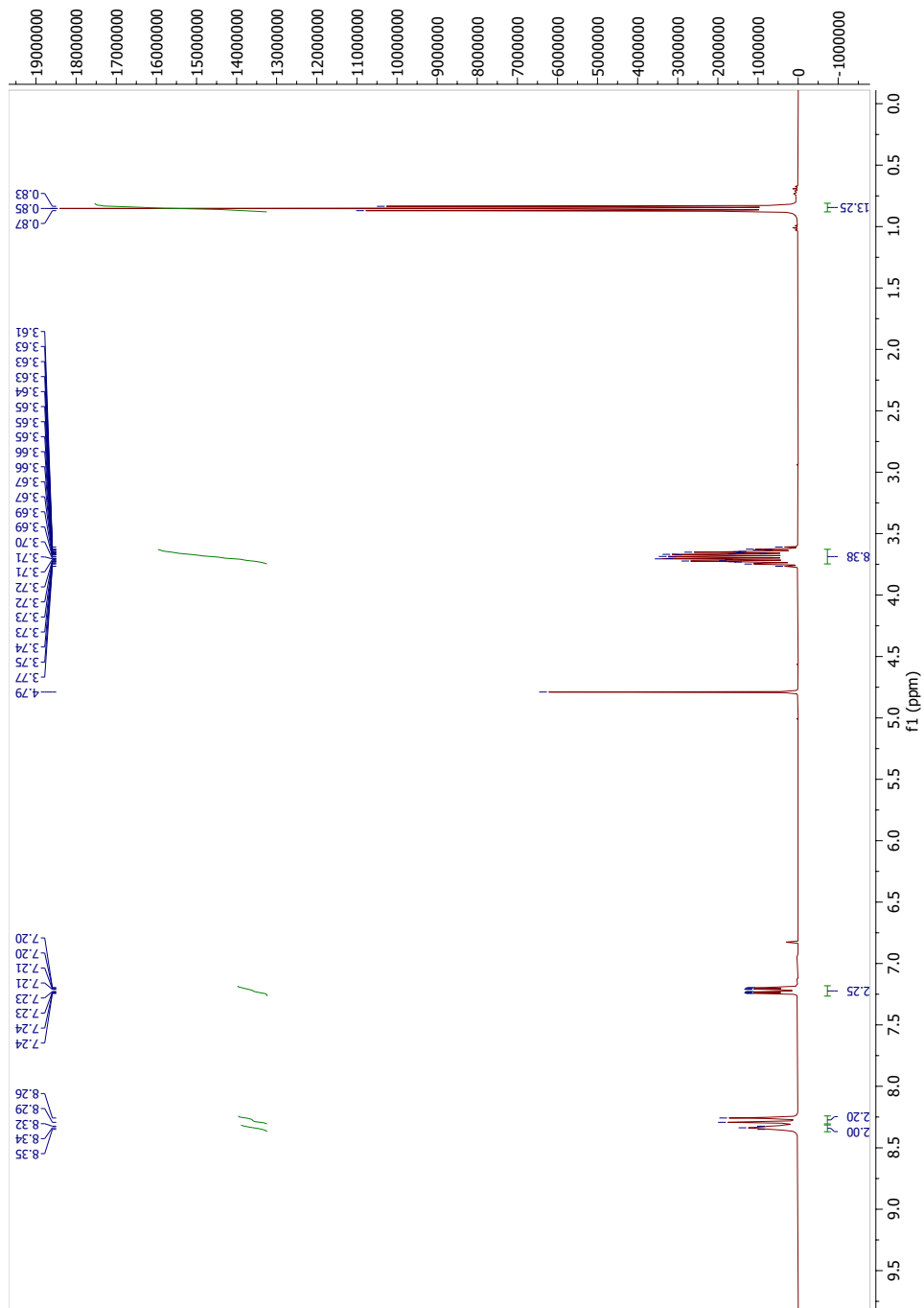


Appendix 5. ^{31}P NMR of **3**

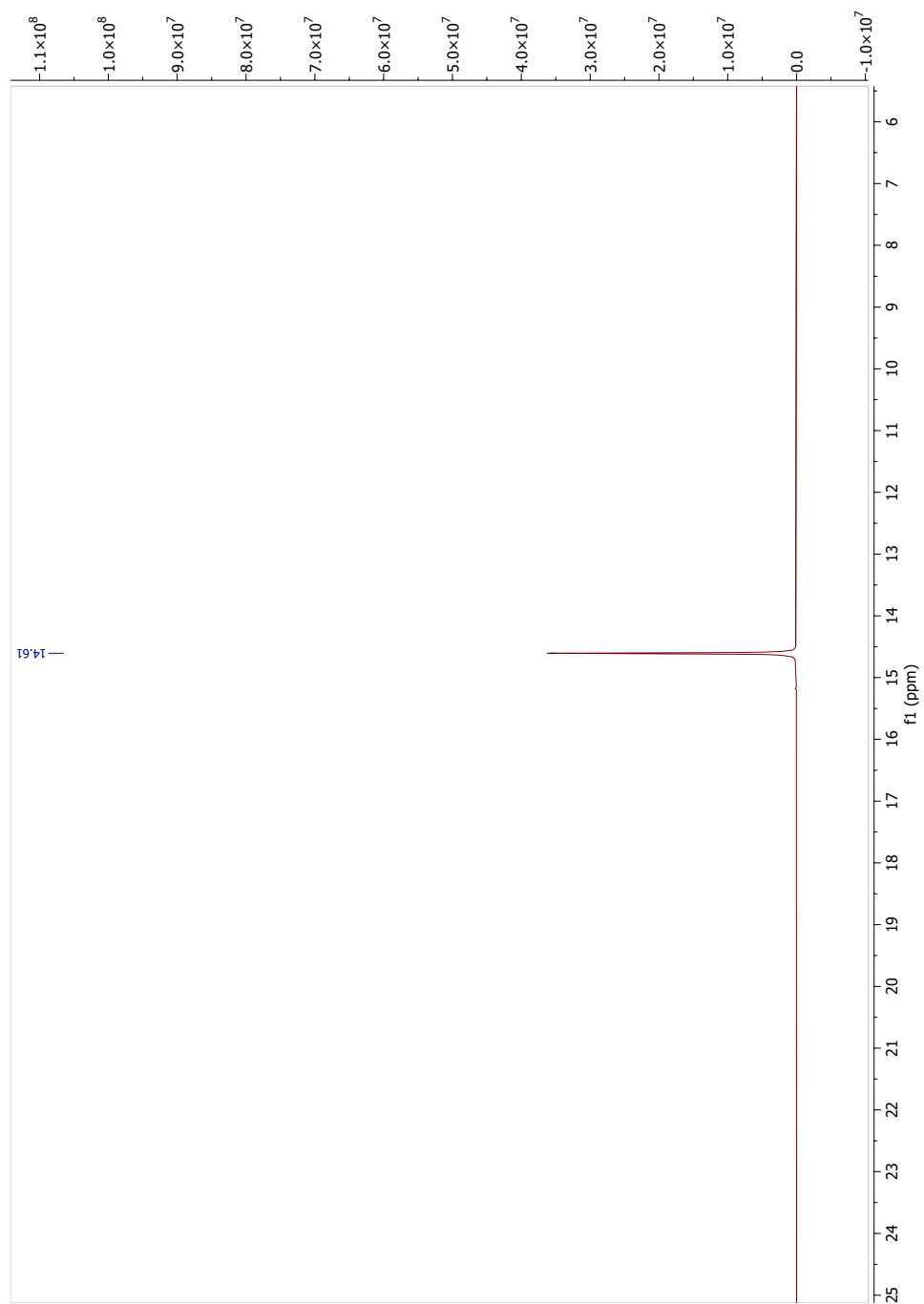


s0'8—

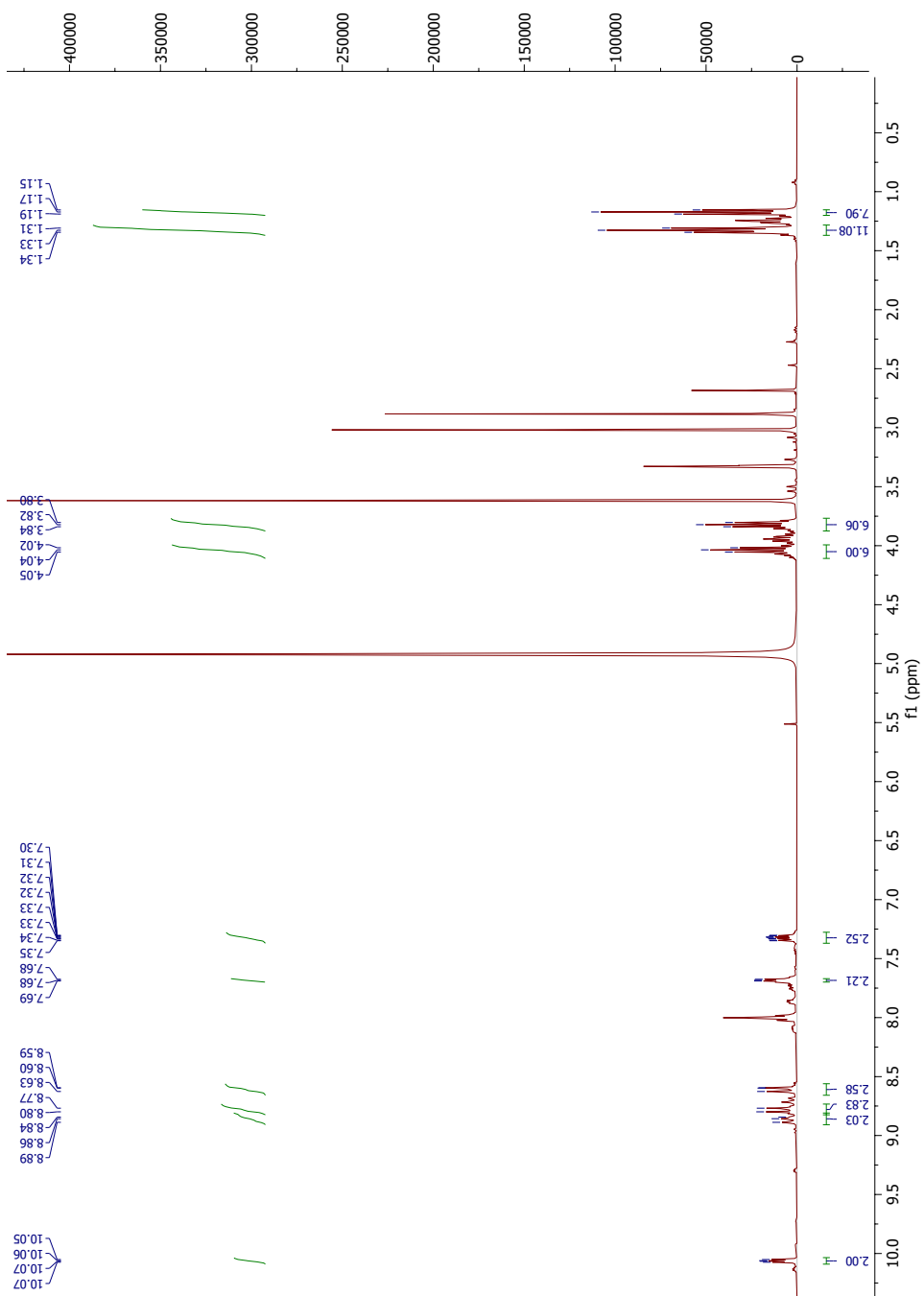
Appendix 6. ^1H NMR of 4



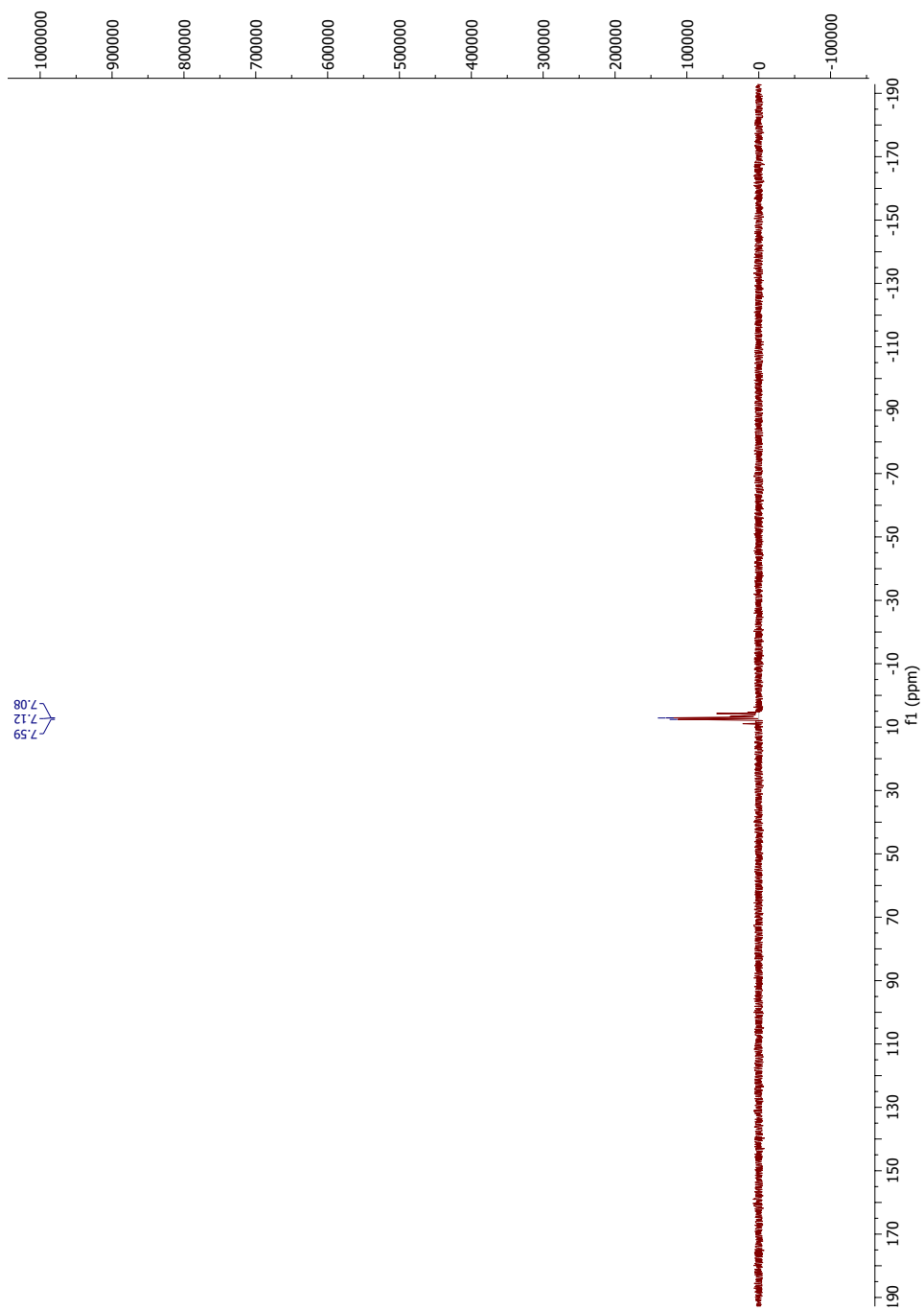
Appendix 7. ^{31}P NMR of **4**



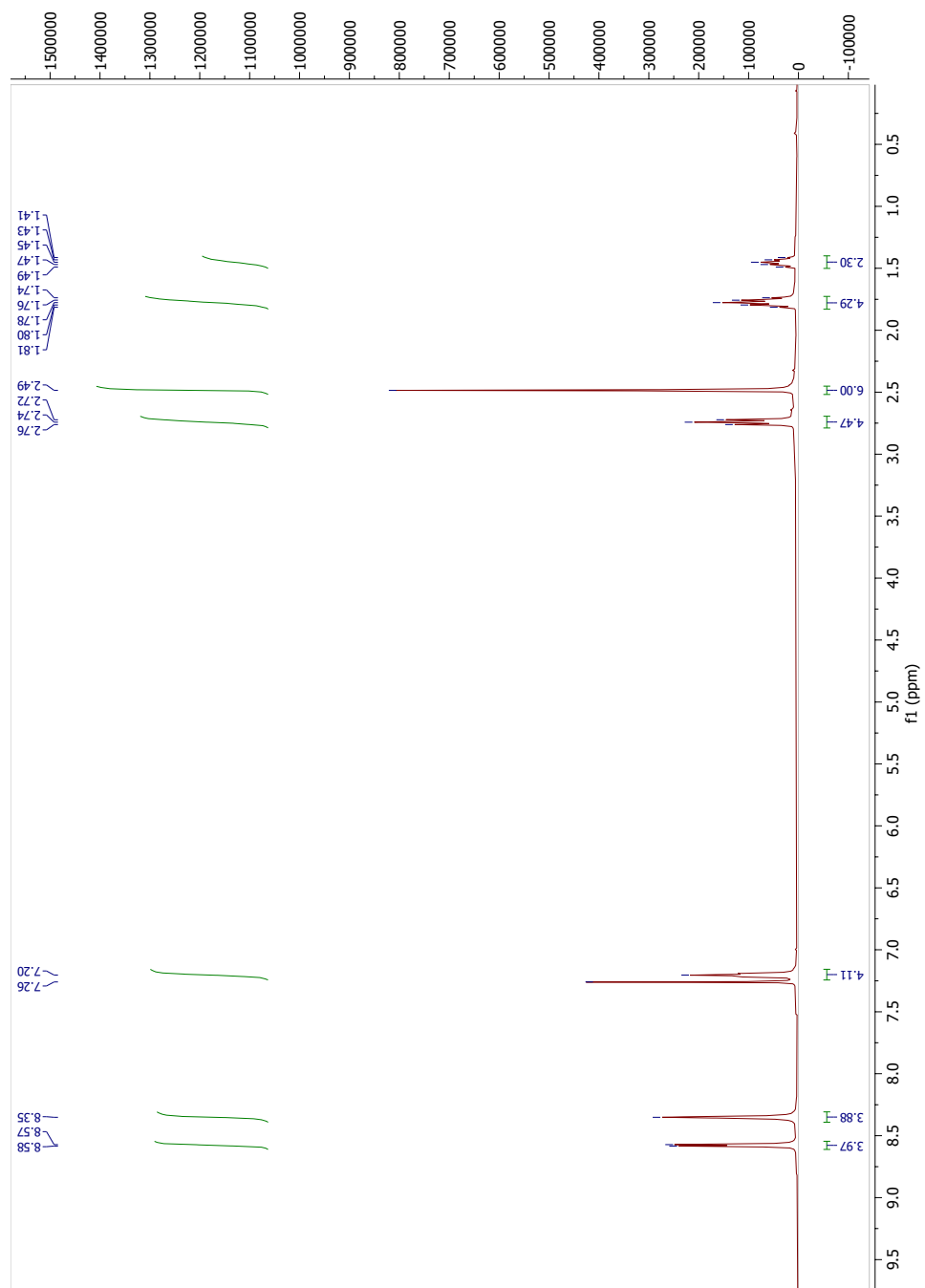
Appendix 8. ^1H NMR of 5



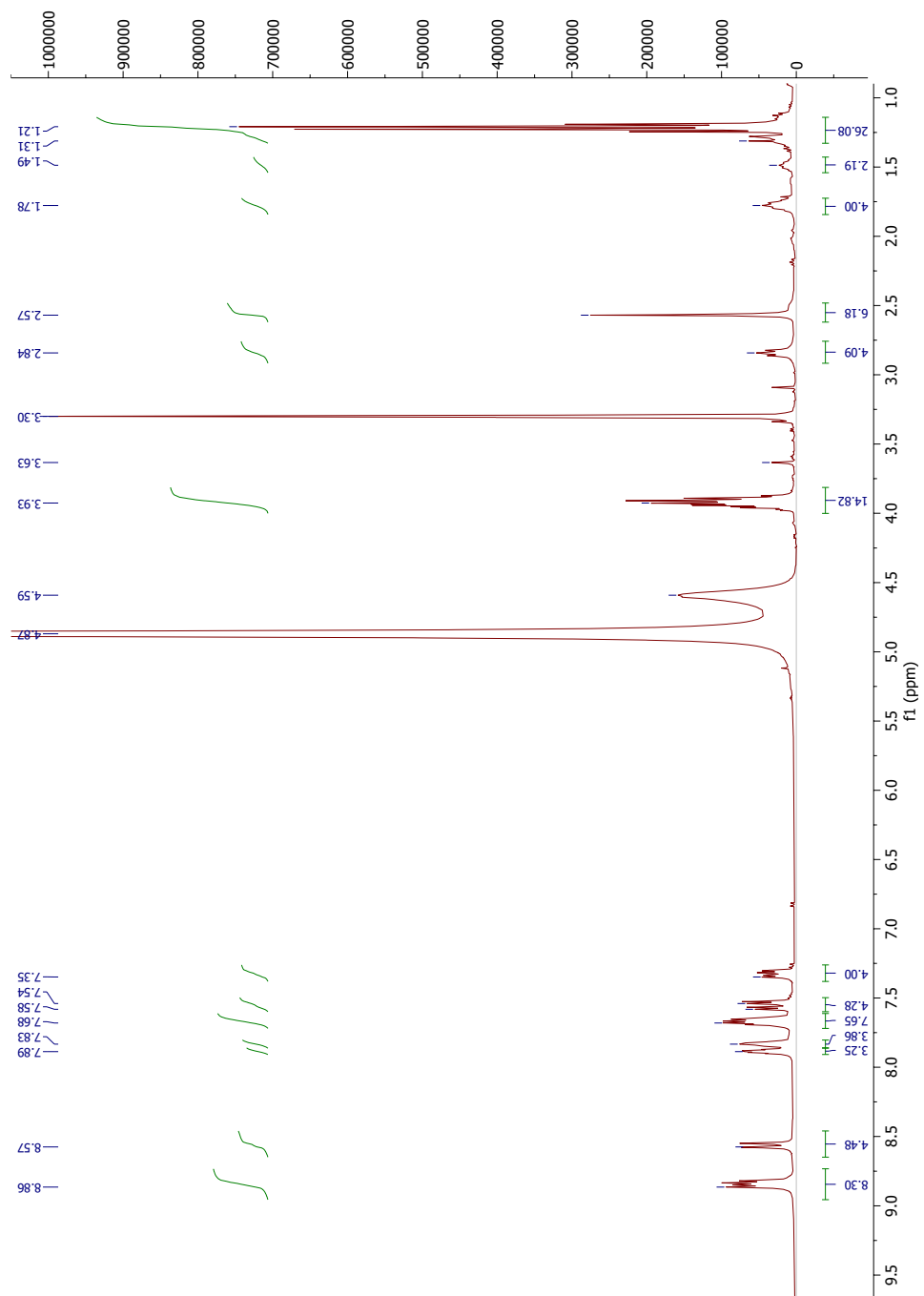
Appendix 9. ^{31}P NMR of 5



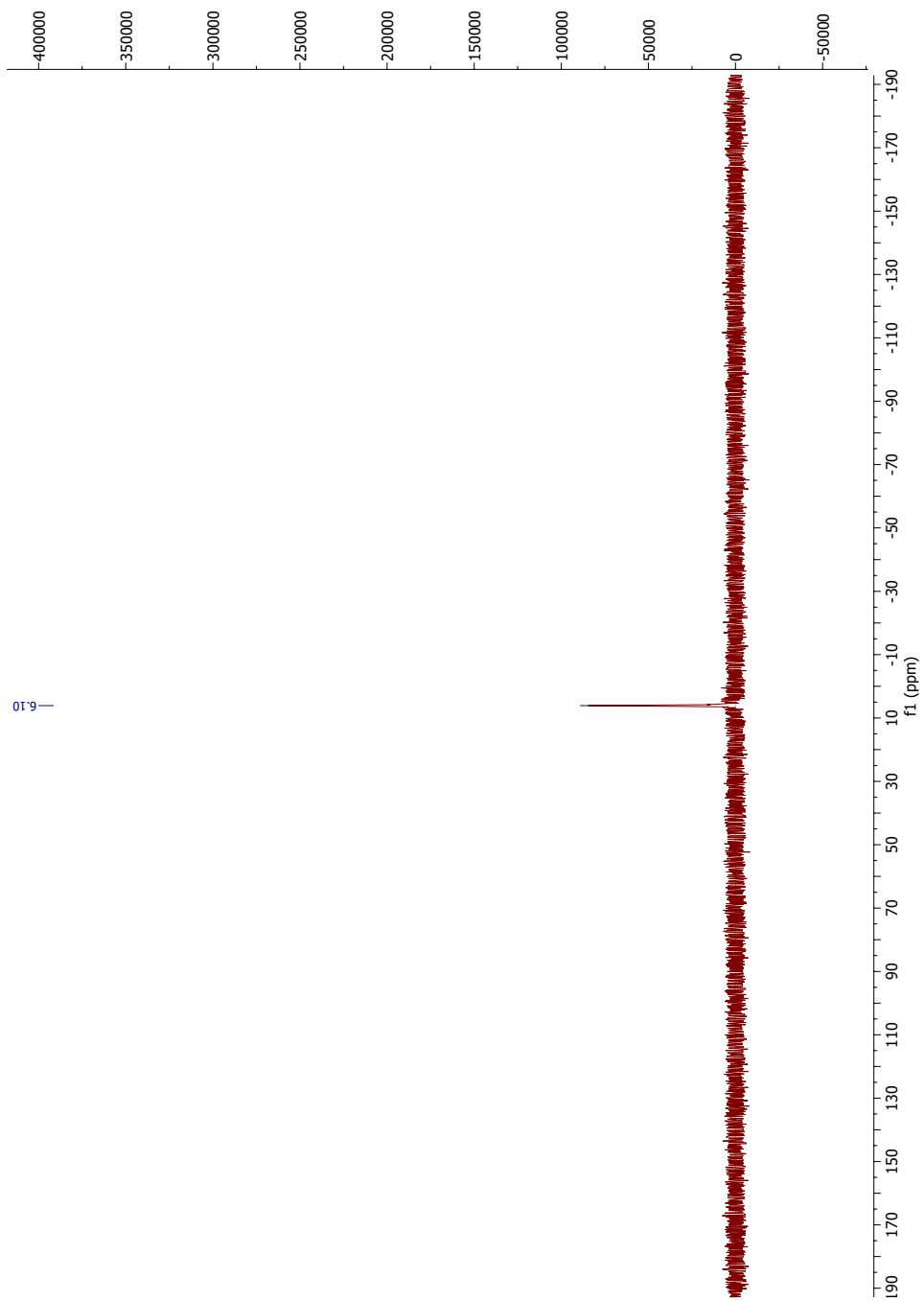
Appendix 10. ^1H NMR of 6



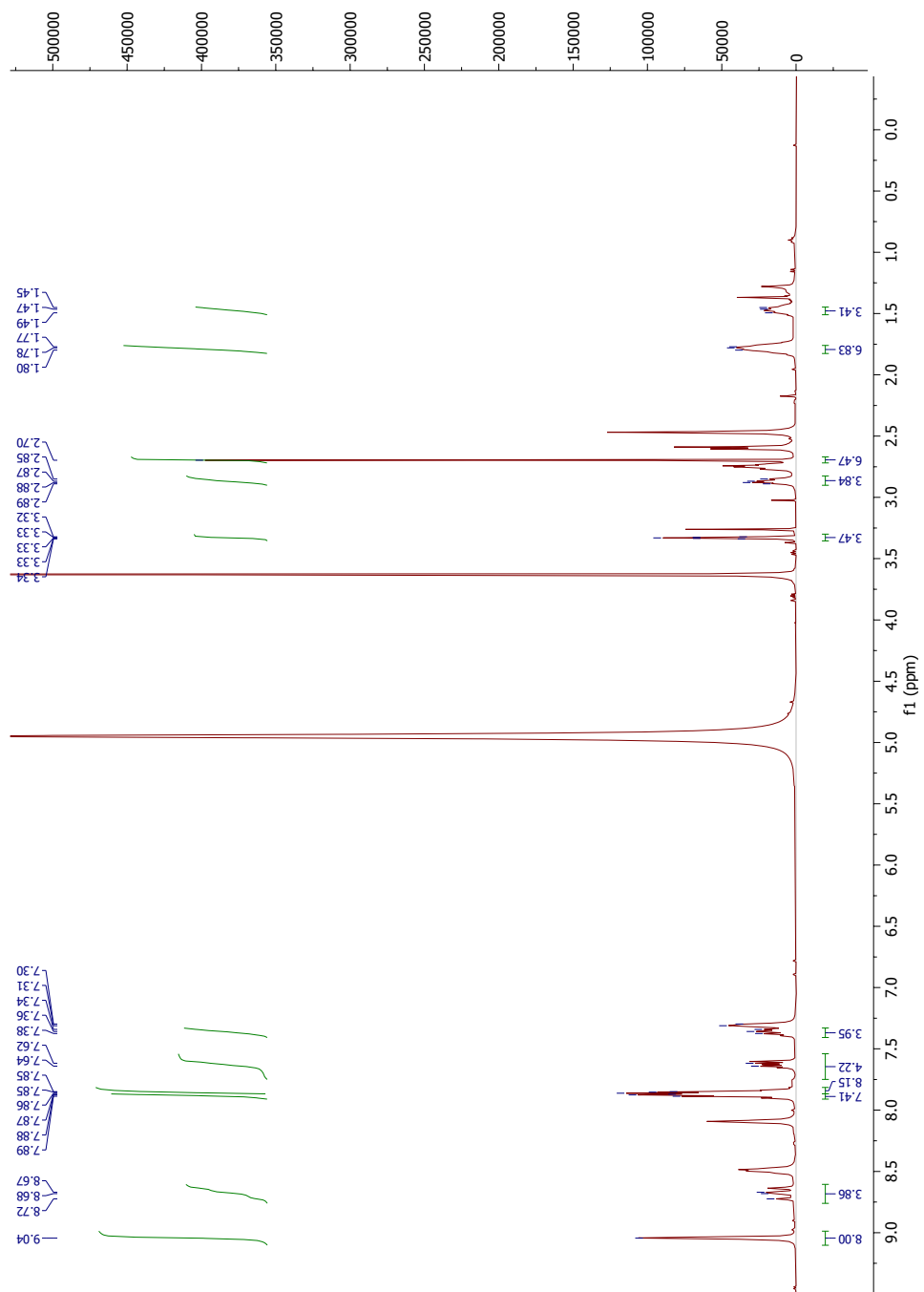
Appendix 11. ^1H NMR of 7



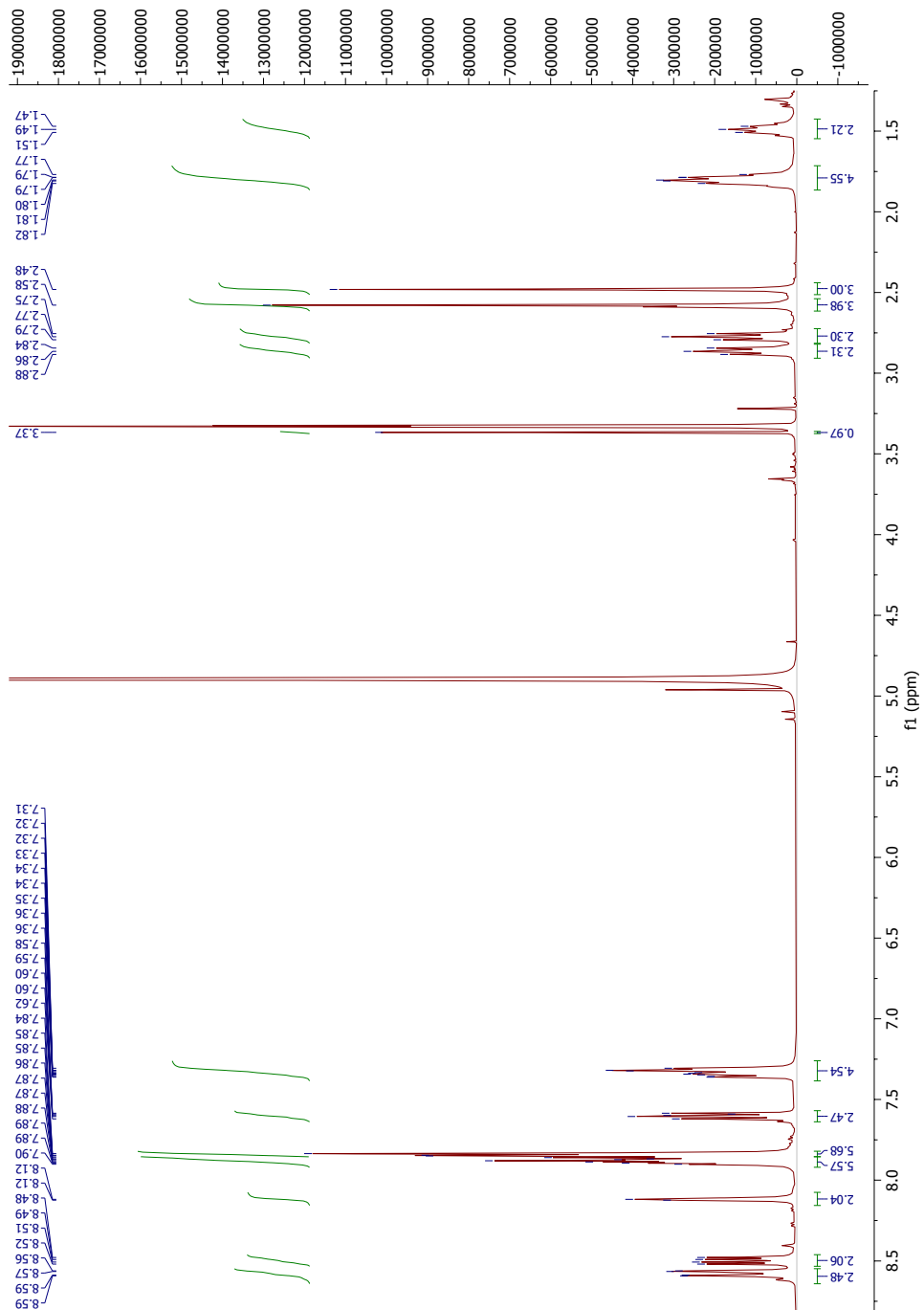
Appendix 12. ^{31}P NMR of 7



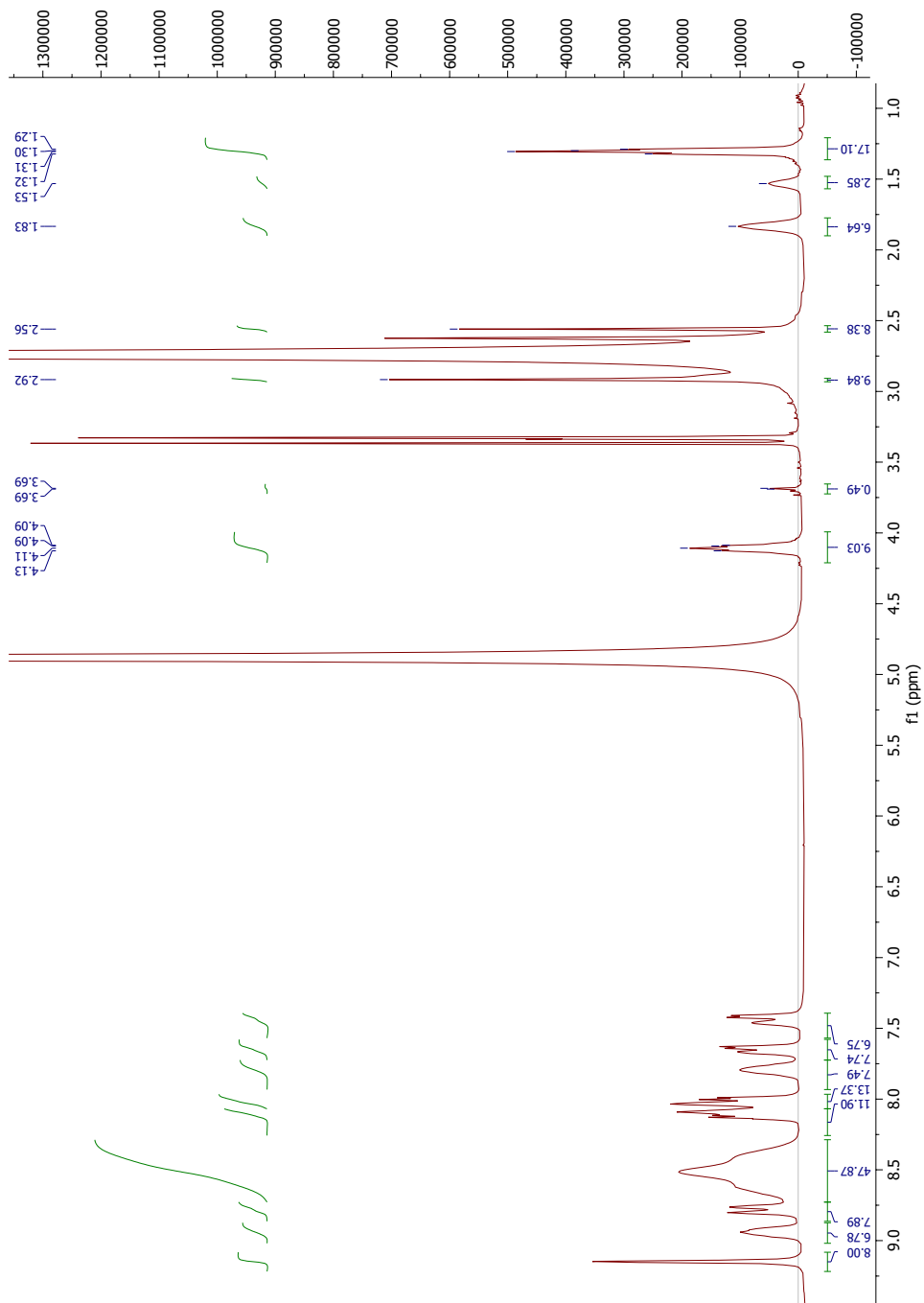
Appendix 13. ^1H NMR of 9



Appendix 14. ^1H NMR of 10



Appendix 15. ^1H NMR of 11



Appendix 16. ^{31}P NMR of 11

